Master's thesis

NTNU
Norwegian University of Science and Technology
Faculty of Engineering
Department of Civil and Environmental Engineering

Mari Gilje Lillegraven

# Hydrological modelling of infiltration swale and local ungauged catchment

## A case study at Rv3 Stabekken

Master's thesis in Civil and Environmental Engineering
Supervisor: Knut Alfredsen and Tone Merete Muthanna
June 2021

NTNU
Kunnskap for en bedre verden

Mari Gilje Lillegraven

# Hydrological modelling of infiltration swale and local ungauged catchment

## A case study at Rv3 Stabekken

Master's thesis in Civil and Environmental Engineering
Supervisor: Knut Alfredsen and Tone Merete Muthanna
June 2021

Norwegian University of Science and Technology
Faculty of Engineering
Department of Civil and Environmental Engineering

NTNU
Norwegian University of
Science and Technology

**NTNU – NORWEGIAN UNIVERSITY OF SCIENCE AND TECHNOLOGY**
**Department of Civil and Environmental Engineering**

TVM 4905 Master thesis in Water and Wastewater Engineering

Candidate: **Mari Gilje Lillegraven**

Subject: Hydrological modelling of infiltration swale and local ungauged catchment at Rv3 Stabekken.

## Background

In connection with the construction of a new national road, Rv3, from Løten to Elverum, swales with high infiltration capacity have been designed along the road. These swales will handle runoff from the road and secure safe stormwater management and treatment of road runoff. This road development is a pilot project in Klima2050. To assess the effect of the swales, measurement instruments have been set up on a section of the swale by Stabekken in Løten, to be able to assess infiltration and transport of water in the swale. This will provide information on how the swale works with different input at different times of the year. A climate station and several pressure sensors have been established at different depths in the swale. As part of project work in the subject TVM4510 (specialisation project), pressure sensors have been installed during fieldwork in Stabekken at a culvert outlet.

The purpose of this task is to model the runoff from the road to the swale, transport of water in the swale and the flow in Stabekken by the culvert outlet. This will form the basis for assessing how efficiently the swale works regarding water quantity reduction and model flow in the local catchment draining into Stabekken.

## Tasks

The assignment will have the following main tasks:

1. Prepare data for analysis. This work will be based on previous project work and may include:
    a. A further assessment of quality in data from climate station and pressure sensors, and a basic analysis of the connection between these.
    b. Quality control and presentation of measurement data collected during the project period.
2. Select and set up a hydrological model for the swale and simulate infiltration into the swale and runoff from the swale. Assess the extent to which measurement data from pressure sensors can be used to calibrate this model.
3. Select and set up a model for the catchment draining in Stabekken at the outlet of the culvert. Look at different approaches to assess the quality of data related to measurement data from pressure cells located in the stream. Evaluate the model's applicability in small ungauged catchments such as Stabekken.

**Guidance, data and information**
Supervisors of this thesis are Professor Knut Alfredsen and Tone Muthanna at the Department of Civil and Environmental Engineering, NTNU. The candidate is otherwise responsible for the collection, control and use of data. Help from the above or others must be referred to in the report.

**Report**
The structure and layout of the report are important. Assume that the target group are technical personnel at senior level. The report must contain a summary that gives the reader information on the background, procedure and main results. The report must have a table of content and a reference list. The reference list must be formatted according to an existing standard.

The format of the report must follow the standard at NTNU. All figures, maps and pictures included in the report must be of good quality with clear text on the axis and legend.

The deadline for submission of the thesis is 11th of June 2021.

Department of Civil and Environmental Engineering, NTNU

Knut Alfredsen
Professor

# Abstract

Floods are associated with negative consequences to infrastructure, environment, economy and people. Climate change increases the frequency and magnitude of extreme rain events, which can lead to floods. Sustainable stormwater management can reduce the quantity and improve the quality of runoff. Infiltration and detention of stormwater will reduce the flood peaks. Estimation of flow in small ungauged catchments serves as a challenge in hydrology due to fast response and a lack of data, making it difficult to assess the accuracy of predicted runoff.

An infiltration grass swale is established to reduce the quantity and pollution of road runoff along a part of the recently opened (July 2020) road Rv3 between Løten and Elverum in Norway. A stretch of a local stream, Stabekken, was rearranged to be located along the road. This study focuses on the hydrological performance of the swale and flood estimation in the small ungauged catchment that drains into Stabekken. This contributes to Klima2050's goal to gather knowledge to reduce floods within built environments.

The swale's hydrological efficiency is evaluated mainly based on available water levels measurements within the swale. A model simulating the swale runoff using Storm Water Management Model (SWMM) is however set up and indicates little runoff during design rain events. Due to a lack of data on outflow and soil properties, the model is not calibrated, making it difficult to conclude whether the swale's hydrological performance is adequate during extreme rainfall events. The water level measurements within the swale indicate infiltration of all road runoff during the monitoring period and dampening of precipitation events. This indicates good performance of the swale, at least during the monitoring period. Infiltration measurements and longer time series are recommended for further evaluation of the swale's hydrological performance, which can be reduced with time and during winter seasons.

Flow in Stabekken is estimated using the recently developed Distance Distribution Dynamics (DDD) model, a parsimonious and continuous model. The prediction accuracy of the model is assessed using available water stage data from Stabekken. There are similarities in timing and relative magnitude of peaks between the simulated discharge and measured water stage. This indicate suitability of the DDD model in Stabekken when using a combined regionalisation method (regression for recession parameters and physical similarity for calibration parameters). Flow data is however not available, which makes no detailed flood magnitude assessment possible. The model is also used to predict flood peaks in different antecedent soil moisture conditions, which generate peaks of different magnitudes. The antecedent catchment conditions are found through simulation, which is possible when using continuous models. Design peak flows modelled in wet conditions are up to 33% greater than flood peaks modelled in dry conditions in Stabekken using the same design precipitation event. Based on these findings, the DDD model is found suitable for flood prediction in Stabekken, a small ungauged catchment.

# Sammendrag

Flom er forbundet med negative konsekvenser for infrastruktur, miljø, økonomi og mennesker. Klimaendringer øker hyppigheten og størrelsen på ekstreme regnhendelser som kan føre til flom. Bærekraftig overvannshåndtering kan redusere mengden og forbedre kvaliteten på avrenningen. Infiltrasjon og forsinkelse av overvann vil redusere flomtoppene. Estimering av vannføring i små umålte felt er en utfordring i hydrologi på grunn mangel på data som gjør det vanskelig å vurdere nøyaktigheten av estimert vannføring.

Det er etablert en gresskledd infiltrasjonsgrøft for å redusere mengden og forurensningen av veiavrenning langs en del av den nylig åpnede (juli 2020) veien Rv3 mellom Løten og Elverum i Norge. En strekning av en lokal bekk, Stabekken, ble lagt om for å ikke krysse veien, men ligge langs veien. Denne studien fokuserer på den hydrologiske ytelsen til veigrøften og estimering av flom i det lille umålte feltet som dreneres til Stabekken. Dette bidrar til Klima2050s mål om å samle kunnskap for å redusere flom i miljøer med bebyggelse og infrastruktur.

Infiltrasjonsgrøfta sin hydrologiske effektivitet vurderes hovedsakelig basert på tilgjengelige vannstandsmålinger i grøfta. En modell som simulerer avrenning fra grøfta ved bruk av Storm Water Management Model (SWMM) er imidlertid også satt opp, og simuleringene indikerer lite avrenning under intense regnhendelser. På grunn av mangel på data om utstrømning og jordegenskaper til materialene i grøfta er ikke modellen kalibrert, noe som gjør det vanskelig å konkludere om grøfta sin hydrologiske ytelse er tilstrekkelig under ekstrem nedbør. Vannivåmålingene fra grøfta indikerer infiltrasjon av all avrenning av veien i måleperioden, samt demping av nedbørshendelser. Dette indikerer god ytelse av grøfta, i det minst under måleperioden. Infiltrasjonsmålinger og lengre tidsserier anbefales for videre evaluering av grøfta sin hydrologiske ytelse, som kan reduseres over tid og under vintersesonger grunnet konsekvenser av kaldt klima.

Vannføring i Stabekken er estimert ved hjelp av den nylig utviklede Distance Distribution Dynamics (DDD) modellen som er en kontinuerlig modell med få kalibrerte parametere. Forutsigelsesnøyaktigheten til modellen blir vurdert ved hjelp av tilgjengelige vannstandsdata fra Stabekken. Det er likheter i timing og relativ størrelse på topper mellom simulert vannføring og målt vannstand. Dette indikerer at DDD-modellen med en kombinert regionaliseringsmetode er egnet for estimering av vannføring i Stabekken. Observert vannføringsdata er imidlertid ikke tilgjengelig, noe som ikke muliggjør en nøyaktig vurdering av estimert flomstørrelse. Modellen brukes også til å forutsi flommer i forskjellige forutgående jordfuktighetsforhold som genererer flomtopper av ulik størrelse. De forutgående feltforholdene blir funnet gjennom simulering, noe som er mulig når kontinuerlige modeller brukes. Ekstremflommer modellert i våte forhold er opptil 33% større enn flomtopper modellert i tørre forhold i Stabekken ved bruk av samme ekstreme nedbørshendelse. Basert på disse funnene er DDD-modellen funnet egnet for flomestimering i Stabekken som er et lite umålt felt.

# Preface

This master's thesis is written during the spring semester of 2021. It is the final product in the course "TVM4905 Water and Wastewater Engineering, Master's thesis", which corresponds to a workload of 30 credits. This is the last course that completes the integrated master programme Civil and Environmental Engineering at the Norwegian University of Science and Technology (NTNU).

The learning outcomes of this thesis are to gain knowledge and experience on data collection and analysis, hydrological modelling of stormwater management solutions and ungauged catchments, and evaluation of hydrologic performance based on available data and modelled results.

Preliminary work, such as installation of instruments and some data collection, model selection and literature reviews, were conducted in a specialisation project during the fall semester of 2020 (Lillegraven, 2020). This work is attached due to being unpublished. Parts of the theoretical background in the following master thesis are based on findings from these literature reviews. This is, however, specified in the particular sub-chapters.

Thank you to my supervisors, Professor Knut Alfredsen and Professor Tone Merete Muthanna at the Department of Civil and Environmental Engineering, NTNU, for providing me with great guidance and support during this work. I will also express my gratefulness to Siri Guldseth, working in the National Public Roads Administration (NPRA), for collecting and sending valuable measurement data from the swale and Stabekken. Thank you to PhD Candidate Elhadi Mohsen Hassan Abdalla for help and guidance with setting up and running the DDD model. I will express my gratitude to Klima2050 for letting me be a part of one of their projects. Lastly, I will like to thank NPRA for financial support, so that I could conduct fieldwork at Rv3.

Mari Gilje Lillegraven
Trondheim, June 2021

# Contents

# List of Figures

# List of Tables

# Abbreviations

| | |
|---|---|
| AADT | Annual average daily traffic |
| CD | Catchment descriptor |
| DDD | Distance Distribution Dynamics (Hydrological model) |
| GNSS | Global Navigation Satellite Systems |
| GI | Green Infrastructure |
| GIS | Geographic Information System |
| HBV | Hydrologiska Byråns Vattenbalansavdeling (Hydrological model) |
| HEC-HMS | Hydrologic Engineering Centre – Hydrologic Modelling System |
| IAHS | International Association of Hydrological Sciences |
| IDF | Intensity-Duration-Frequency |
| LID | Low Impact Development |
| MET | Norwegian Meteorological Institute |
| NPRA | The National Public Roads Administration |
| NVE | Norwegian Water and Energy Directorate |
| NTNU | Norwegian University of Science and Technology |
| OUH | Overland flow unit hydrograph |
| PUB | Prediction in Ungauged Basins |
| SUDS | Sustainable Urban Drainage Systems |
| SWMM | Storm Water Management Model |
| UH | Unit Hydrograph |

# 1 Introduction

Climate change has hydrological impacts as it increases the magnitude and frequency of heavy rainfall events, which lead to floods. Floods are associated with severe consequences to infrastructure, people, the economy and the environment. Infrastructure systems are designed to be operational for an extended period. Hence, knowledge on climate change's hydrological impacts on both planned and existing infrastructure is essential (Balston et al., 2017).

Surface runoff, also called stormwater, is the part of the rainfall that runs off from impervious surfaces and does not evaporate or infiltrate into pervious surfaces. Rainfall and catchment characteristics are closely connected to the quantity and quality of surface runoff. The focus on sustainable stormwater management has increased considerably in the last decades due to the effects of climate change and urbanisation, which lead to more and faster runoff from impervious surfaces, which can generate floods. Multiple terms are used for infrastructure that provide sustainable stormwater management, such as Low Impact Development (LID), Sustainable Urban Drainage Systems (SUDS) and Green Infrastructure (GI). LID is used in this thesis as practices that control stormwater close to the source through infiltration and detention of precipitation, and safe transport of stormwater (Damodaram et al., 2010). Quality improvement of stormwater can also be achieved in LIDs, which is favourable to prevent pollution of receiving waters. LID establishment can reduce the quantity and peak of runoff, which prevent flooding.

Grass swales are LIDs designed mainly to infiltrate smaller rain events and provide safe stormwater transport through velocity and volume reduction of runoff (Davis et al., 2012; Rushton, 2001). A grass swale will change the flow response in surrounding catchments due to runoff peak reduction. The hydrological performance of a swale is essential for its influence on the flow response in surrounding catchments.

The flow response in a catchment depends, among other things, on its size. Catchments less than 50km$^2$ are defined as small catchments in Norway (Fleig & Wilson, 2013). The hydrological response in such catchments is more variable and different than in larger catchments. The uncertainty in flood estimation methods for small catchments is high due to fast response and flow accumulation. Another challenge associated with flood estimation is the unavailability of flow data. Flow data is essential when predicting floods with acceptable accuracy. Most catchments are however ungauged, meaning no observed streamflow data is available. The International Prediction in Ungauged Basins (PUB) initiative in 2003-2012 was launched by the International Association of Hydrological Sciences (IAHS) to increase the knowledge and focus on PUB and reduce the uncertainty in flood predictions (Sivapalan et al., 2003). Suitable rainfall-runoff models and regionalisation methods were recommended for flood estimation in ungauged catchments. Due to the uncertainties associated with both small

and ungauged catchments, accurate flood estimation in small ungauged catchments is a challenge in hydrology.

## 1.1 Study objectives

This thesis aims to evaluate and model the water transport in the water management systems established along a new road (Rv3 Stabekken). The study is a part of Klima2050's project on sustainable stormwater management at Rv3. A grass swale is established to reduce the quantity and improve the quality of road runoff. Measurement data on the water levels within the swale are available and will be used for evaluation. Stabekken, a local ungauged stream close by the swale, was rearranged during the establishment of Rv3. A hydrological model suitable for flow estimation in small ungauged catchments will be used to model flow in Stabekken, and available water stage data will be used to evaluate the model's applicability.

The original objective was to model the water transport in the infiltration swale and its interaction with the surrounding catchment to predict floods in the small catchment. Due to some discrepancies between the planned and built system, the original objective was modified to hydrological modelling and evaluation of the infiltration swale and local catchments separately. The particular discrepancies are further described in chapter 3.

Two main objectives are defined. Sub-points are included to define the more detailed objectives of the thesis.

- Evaluate the hydrological performance of the infiltration swale established along Rv3.
    - Set up and test a hydrological model that includes the road runoff and the swale.
    - Use the model and the available measurement data to evaluate the hydrological performance of the swale.
- Set up and test a hydrological model of the rearranged part of Stabekken using the DDD model and evaluate its applicability for flood estimation in small ungauged catchments.
    - Estimate flow peaks in Stabekken in different antecedent soil moisture conditions.
    - Evaluate the model's applicability in Stabekken using measured water stage data.
    - Estimate and evaluate the channel stability in the rearranged part of Stabekken during predicted flood peaks.

## 1.2 Structure of the thesis

The thesis is structured as follows:

**Chapter 1 – Introduction:** A general introduction and background on stormwater management and flood prediction, and a description of the study's objectives.

**Chapter 2 – Theoretical background:** Theory on concepts essential to understand and develop the methods for addressing the objectives is presented. A summary from a literature review conducted by (Lillegraven, 2020) on grass swales focusing on hydrological performance and the effect of cold climates is given. Findings from a

literature review by Lillegraven (2020) on flood estimation in ungauged catchment and regionalisation methods are presented. Then, the chosen model approaches in this study are described, and a description of the recently developed DDD model structure is given. Theory on erosion processes and channel stability are presented at the end of this chapter.

**Chapter 3 – Study area:** The study area and the installed stormwater management systems are described. Detected discrepancies between the planned and built solutions are described.

**Chapter 4 – Materials and methods:** The materials and methods used to address the objectives of the study are described. This includes the instrumental setup at the study site, determination of design rain events used in modelling, the model set up and parameters selection of both models used for hydrological modelling of the swale and Stabekken, and lastly, the method for determination of channel stability in the stream.

**Chapter 5 – Results and discussion:** The results and discussion are included in the same chapter since this is found most suitable for this particular study. Model results and data analysis are presented, and the models and evaluation of the studied systems are discussed.

**Chapter 6 – Conclusions**: Conclusions on all objectives are summarised, and recommendations for future work are presented.

# 2 Theoretical background

This chapter includes findings from literature reviews done on grass swales in cold climates and flow estimation in ungauged catchments, including regionalisation methods, conducted during the specialisation project (Lillegraven, 2020). The model approaches used in this master thesis and a thorough description of the model used for one of the modelling purposes, which is developed in the last decade, are given. The chapter ends with theory on erosion processes and channel stability.

## 2.1 Grass swales

The main functions of a grass swale are slow and safe conveyance of stormwater, infiltration of small rain events and reduction of the stormwater quantity. Stormwater quality improvement can also serve as a function of a grass swale if it is designed with this intention, using a filter under the surface that treats the infiltrated water. However, stormwater treatment in grass swales will not be the focus of this brief background on grass swales.

A literature review on grass swales and their performance where conducted during the specialisation project (Lillegraven, 2020). A summary of the findings is presented in this sub-chapter. It was found that the hydrological performance of swales is mainly influenced by design factors such as the impervious drainage area, longitudinal slope and rain event (Winston et al., 2017). The longitudinal slope of the swale has a significant impact on the flow features, which are essential for the extent of stormwater volume reduction and erosion in the swale. The flow can be subcritical or supercritical. Supercritical flow reduces volume retention and increases erosion in the swale, which should be avoided. Subcritical flow is favourable and obtained through sufficient hydraulic resistance in the swale. Specific design elements that increase the hydraulic resistance are stones, check dams and grass coverage (Davis et al., 2012; Mishra et al., 2006; Monrabal-Martinez et al., 2018; Narsimlu et al., 2004).

Grass species with deep roots are recommended as vegetation in a grass swale due to stabilising effects, keeping the topsoil layer bound. Thus, the soil is protected from erosion of flow with small velocities. The grass will deflect, and the hydraulic resistance decrease during flood events if the flow depth and velocity increases. However, the soil layer is protected from erosion due to grass deflection. Grass species will also maintain another desirable effect, namely the swale's infiltration capacity, which is essential for volume reduction of stormwater in the swale (García-Serrana et al., 2017).

### 2.1.1 Cold climate's influence on grass swales

Winter times in cold climates affect the performance and operation of LIDs, such as grass swales, due to low temperatures and snow. Few guidelines have specific design criteria for swales in cold climates. The conditions, which the general guidelines are based on, are however different from winter conditions in cold climates.

Water infiltrates into frozen ground, provided that the initial soil moisture is low when the soil freezes. If the water content in the soil is high during low temperatures, concrete frost occurs, leading to no infiltration of stormwater or snowmelt (Muthanna et al., 2007). A study by Fach et al. (2011) investigated the performance of grass swales during winter times in the Alpine region and found that the drainage capacity was significant for the performance of the swale. Hence, sufficient drainage of grass swales will avoid concrete frost and maintain infiltration and volume reduction of stormwater and snowmelt during winter.

During winter, swales are valuable for snow management as they are suitable for snow storage (Caraco & Claytor, 1997). However, this can decrease the hydrological swale performance due to deposition of sediments and pollutions that accumulate in the snow. Fach et al. (2011) observed deposition of gravel and fine particles that lead to a distinct decrease in the swale's infiltration capacity and hydrologic performance. Inspection and maintenance of swales, such as removing residual sediments, are essential, particularly after snowmelt, to maintain an efficient grass swale (Caraco & Claytor, 1997). Despite the decreased performance of swales during winter times in cold climates, the operation was found sufficient according to guidelines (Fach et al., 2011). The reason may be less intense precipitation during winter and that the swales are designed based on precipitation data which include heavy rain events that occur during summer.

## 2.2 Flow estimation in ungauged catchments

Chapter 2.2. and 2.3 summaries findings from a literature review conducted in the specialisation project on flow estimation and regionalisation methods used in ungauged catchments (Lillegraven, 2020).

Estimation of floods can be obtained using different methods. Hydrological models can avoid subjective assumptions and provide complete hydrograph characteristics, which are limitations associated with statistical floods estimation methods (Wilson et al., 2011). Hydrological models are simplified representations of the physical processes in hydrology and the interaction between them, such as precipitation and infiltration. The best models are those that generate results closest to reality with the least model complexity (Devia et al., 2015). Rainfall-runoff models are common types of hydrological models. They have several possible applications due to runoff being the final result of hydrological processes within a catchment (Parajka et al., 2013). Flow prediction based on forecasted precipitation events and studying impacts of climate change and land-use change on runoff regimes are examples of applications of rainfall-runoff models. Different criteria are used to classify rainfall-runoff models (Devia et al., 2015):

- Equations (empirical, conceptual or physical)
- Model structure (lumped or distributed)
- Output randomness (deterministic or stochastic)
- Time dependency (steady or unsteady)

Flow estimation in ungauged catchments is another application of rainfall-runoff models. The issue of flood prediction in ungauged catchments can be approached using model-independent

or model-dependent methods. The former is entirely data-driven empirical methods, such as scaling. Model-dependent methods, also called regionalisation methods, use hydrological models in the flow estimation process (Razavi & Coulibaly, 2013). In the following sub-chapters, scaling and three common regionalisation methods (physical similarity, spatial proximity and regression) are briefly described.

### 2.2.1 Scaling (Model-independent method)

Scaling is widely used in practical fields in Norway. A scaling factor scale a flow time series from a gauged to an ungauged catchment. The scaling formula is as follows:

$$Q_{UG} = \left(\frac{A_{UG} * F_{UG}}{A_G * F_G}\right) Q_G \tag{2.1}$$

where $Q_{UG}$ and $Q_G$ are the discharge values in the ungauged and gauged location respectively, $A_{UG}$ and $A_G$ are the ungauged and gauged catchment areas respectively, and $F_{UG}$ and $F_G$ are the specific runoff in the ungauged and gauged catchment respectively (Fleig & Wilson, 2013).

Two assumptions are made when using the scaling method to estimate flow in ungauged catchments:

- Similar response to rain events in both catchments
- Equal amounts of rainfall with equal intensity are received in both catchments at the same time.

These assumptions are not easily fulfilled and require the catchments to be similar in location and physical properties. Hence, scaling is not suitable for flow estimation in many ungauged catchments. However, when the assumptions are fulfilled, scaling is preferred as it gives satisfactory results and requires little computation.

## 2.3 Regionalisation (Model-dependent methods)

Regionalisation approaches are model-dependent methods used to deal with the issue of flow prediction in ungauged catchments. The common definition of regionalisation are processes that transfer hydrologic information, e.g. model parameters, from gauged to ungauged catchments (Blöschl & Sivapalan, 1995). Rainfall-runoff models use regionalisation methods to estimate the model parameters when predicting floods in ungauged catchments.

There are several different regionalisation methods. Catchment descriptors are used in regionalisation methods, hence the best approach varies in different catchments and regions. The procedure used in regionalisation studies includes collecting available data, selecting proper regionalisation method(s), performance validation on gauged catchments, and uncertainty analysis (Razavi & Coulibaly, 2013). PUB focused on reducing predictive uncertainty since the regionalisation processes have various sources of uncertainty (Sivapalan et al., 2003). The prediction results of flow in ungauged catchments improve if the uncertainty decreases.

Physical similarity, spatial proximity and regression are commonly used regionalisation methods and are briefly described in the following sub-chapters.

### 2.3.1 Physical similarity

This method transfers unchanged model parameters from similar gauged to ungauged catchments. The first step of this regionalisation approach includes a similarity assessment between the ungauged catchment and the gauged donor catchments based on catchment descriptors. Ranking and similarity index method are commonly used techniques of similarity assessment.

In the ranking method, all donor catchments are ranked based on their catchment descriptors, and the catchment ranked on top has the most similar descriptors as the ungauged catchment. Each catchment descriptor is ranked separately. Hence, the donor catchment with the lowest total rank is the most similar to the ungauged catchment, and its parameter set is transferred to the ungauged catchment (Oudin et al., 2008).

In the similarity index method, the similarity between the donor catchments and the ungauged catchment is assessed using the following formula:

$$SI = \sqrt{\sum_{j=1}^{J} \left( \frac{x_{a,j} - x_{b,j}}{\sigma_{x,j}} \right)^2} \tag{2.2}$$

where $SI$ is the similarity index, $j$ is the number of selected catchment descriptors, $x_{a,j}$ and $x_{b,j}$ are the values the $j$-th catchment descriptor in respectively the ungauged and gauged catchment, and $\sigma_{x,j}$ is the standard deviation of the $j$-th catchment descriptor for all catchments, both ungauged and gauged.

A small value of indicates that the donor catchment is similar to the ungauged catchment. One or more donor catchments can be used for regionalisation of the model parameters. When using a single donor, the gauged catchment with the smallest similarity index is chosen. If parameter sets from more than one donor catchments are used, it is called a pooling group (Oudin et al., 2008; Tsegaw, Alfredsen, et al., 2019).

### 2.3.2 Spatial proximity

This method assumes that only spatial distance cause variations in parameter values. Similar climate and physical characteristics of the region are also assumed. Model parameter sets are transferred to the ungauged catchment through spatial interpolation techniques when using the spatial proximity method. Kriging is an example of a commonly used interpolation technique (Razavi & Coulibaly, 2013).

### 2.3.3 Regression

This method uses empirical equations to estimate model parameters for ungauged catchments. The equations are based on catchment descriptors. Regression is classified as one-step or two-step regression. The latter is the most used type and includes modelling all donor catchments, extracting calibrated parameter sets, and finding a relation between the catchment descriptors and the calibrated parameters.

## 2.4 Model approach

Two different hydrological models are used in this study, one simulating the swale runoff and another estimating the flow in the local catchment. Brief descriptions of the model choice processes are presented in the following sub-chapters.

### 2.4.1 Model choice for modelling the swale

For choosing what model to use for modelling the swale, a brief evaluation of two hydrological models is done. A preliminary search showed that the Hydrologic Modelling System (HEC-HMS) and Storm Water Management Model (SWMM) are potentially suitable models, and their applicability for modelling the swale is evaluated.

HEC-HMS was developed by the US Army Corps of Engineers at Hydrologic Engineering Centre. The model is designed to simulate the hydrological processes of dendritic catchment systems. It describes the catchment behaviour and simulates the hydrological response. HEC-HMS is made to model hydrographs for a network of watersheds and is most suitable for modelling dendritic catchment systems of a larger size (Kaykhosravi et al., 2018).

SWMM is a distributed rainfall-runoff model and consists of several different blocks or modules. It was developed by the US Environmental Protection Agency and is a widely used rainfall-runoff model that can simulate both single storm events and long-term continuous precipitation (Rossman, 2015). SWMM has a LID module that includes eight predefined LID controls. Hence LIDs can be modelled explicitly in SWMM. HEC-HMS does not have predefined LIDs and has not been widely used for LID modelling purposes (Kaykhosravi et al., 2018). However, LIDs can be modelled implicitly in HEC-HMS, but this is more complex than in models with predefined LIDs such as SWMM. Based on this and that the particular catchment in this study is a small catchment, and has a swale which is a LID, SWMM is found most suitable for this specific modelling purpose.

### 2.4.2 Model choice for modelling flow in Stabekken

A literature review on models appropriate for estimating flow in small ungauged catchments was computed during the specialisation project (Lillegraven, 2020). Hydrologiska Byråns Vattenbalansavdeling (HBV) model and Distance Distribution Dynamics (DDD) model and their applicability were evaluated. There are similarities between HBV and DDD in the structure of the models, but the runoff dynamics and number of parameters that needs calibration are different in the two models. DDD is a parsimonious model, and HBV is an overparameterised model. Through the literature review conducted in the specialisation project (Lillegraven, 2020), the DDD model was found most appropriate for modelling the flow in Stabekken, which is a small ungauged catchment. Tsegaw, Skaugen, et al. (2019) recommended adding a dynamic river network in the DDD modelling routine to increase the prediction accuracy of the flood peaks. Hence, the DDD model with a dynamic river network will be used for modelling the flow in Stabekken.

Since the DDD model is a recently developed model, a thorough description of the model structure is given in the following sub-chapter.

## 2.5 DDD model structure

The DDD model is a conceptual rainfall-runoff model developed in Norway by Skaugen and Onof (2014). The model was developed aiming to reduce the number of calibrated parameters while maintaining the accuracy of the estimated flow. This will result in less uncertainty in the model's structure and parameters (Skaugen & Onof, 2014). It is a parsimonious model where most parameters are related to catchment descriptors and observed runoff characteristics (Skaugen & Weltzien, 2016). Hence, most model parameters can be derived for ungauged catchments. The DDD model is a semi-distributed model, distributed in input data (areal precipitation and temperature) and lumped in model parameters (Tsegaw, Skaugen, et al., 2019).

The DDD model has three main modules (as illustrated in Figure 2.1): Snow, subsurface and runoff dynamics. The snow routine is equal to the snow routine in HBV, where the catchment is divided into 10 elevation zones, and the computations are done in each zone. DDD differs from HBV in its description of the subsurface and runoff dynamics (Skaugen et al., 2015). The subsurface module is divided into unsaturated and saturated zone. The parameters in the runoff dynamics are derived from recession analysis of observed runoff (Skaugen & Onof, 2014).

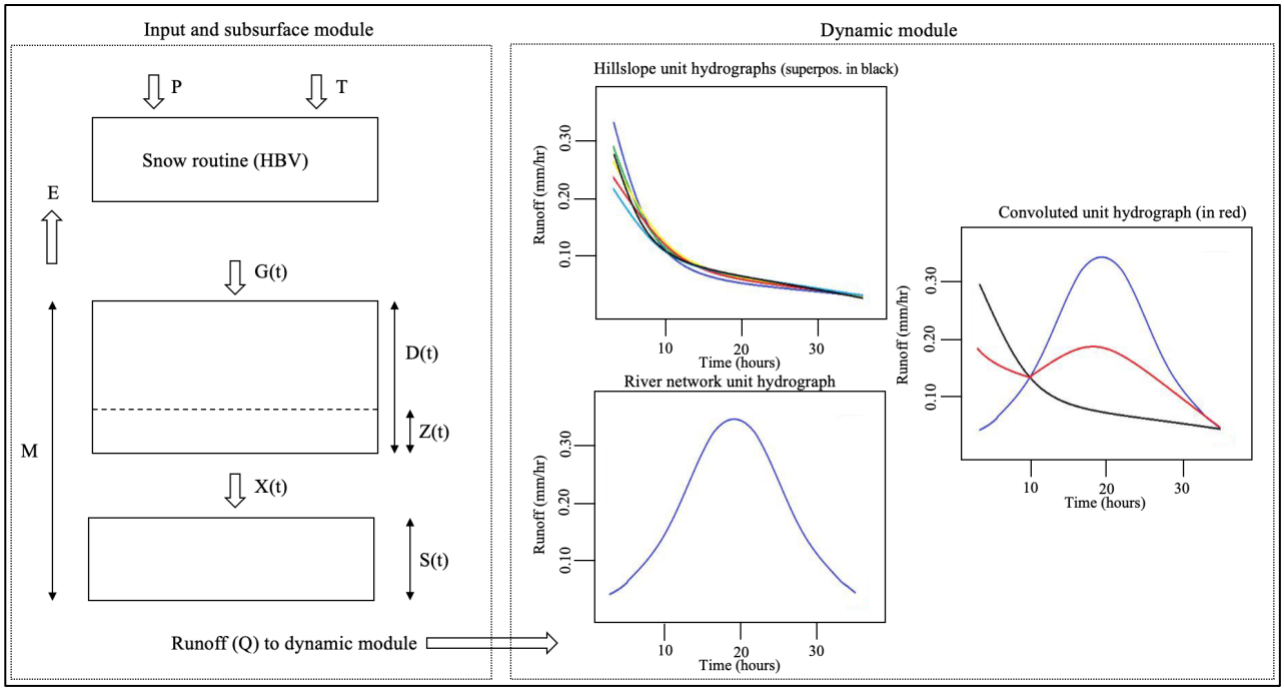


Figure 2.1 General structure of the DDD model (Adapted from Skaugen and Onof (2014)).

### 2.5.1 Precipitation, temperature and snow routine

Areal, gridded precipitation and temperature are inputs to the DDD model and must be calculated before modelling. The catchment is divided into 10 elevation zones, and the areal precipitation and temperature are calculated directly for each zone. This is done by averaging the gridded input data located within the zone. If the catchment is too small so that a zone has

no gridded input, the same input values as the closer zone in elevation are directly assigned to the particular zone. The snow routine in the DDD model is similar to the snow routine in the HBV model. The degree-day model is used for snowmelt and refreeze. *CX*, *CFR* and *PRO* are the calibrated parameters in the snow routine in DDD, as *Tx* and *Ts* are fixed to 0.5°C and 0°C, respectively (Skaugen & Weltzien, 2016). The areal precipitation (*P*) and temperature (*T*) are inputs to the snow routine, and the water released from the snow routine (*G(t)*) is the input in the subsurface routine, as shown in Figure 2.1. The number of calibrated parameters in the snow routine in DDD are reduced compared to HBV since *Tx* and *Ts* are fixed in the DDD model.

### 2.5.2 Subsurface routine

The subsurface in the DDD model includes a tank (*M*) divided into a saturated zone (*S*) and an unsaturated zone (*D*). Released water from the snow routine (*G(t)*) enters the unsaturated zone (*D(t)*), and excess water (*X(t)*) enters the saturated zone (*S(t)*). It becomes runoff if the actual soil moisture, including the received input (*G(t)*) and the existing soil moisture (*Z(t)*), exceeds a threshold (*R*) which describes the field capacity of the soil. The threshold (*R*) is fixed at 30% as it is found to be a reasonable value (Skaugen & Onof, 2014). A degree-day model is used to estimate the potential evapotranspiration (*Epot*) in the DDD model. The degree-day factor (*Cea*), which is positive for positive air temperatures (*Ta*) and zero for negative air temperatures, is the only calibrated parameter in the subsurface routine. The actual evapotranspiration (*Ea*) is estimated as a function of the potential evapotranspiration and soil moisture. The elements in the subsurface routine and the calculations are summarised in Equation (2.3-2.5).

Excess runoff: $$X(t) = \mathrm{Max}\left\{\frac{\mathrm{G(t)+Z(t)}}{D(t)} - R, 0\right\} D(t) \quad (2.3)$$

Potential evapotranspiration: $$Epot = \mathrm{Min}\,\{\mathrm{Cea} * \mathrm{Ta},\ 0\} \quad (2.4)$$

Actual evapotranspiration: $$Ea = Epot * \frac{S+Z}{M} \quad (2.5)$$

### 2.5.3 Runoff dynamics

All parameters in the runoff dynamics in the DDD model are derived from catchment characteristics combined with recession analysis of the observed runoff. The distance distribution derived by a Geographical Information System (GIS) is essential for describing the runoff dynamics of a catchment. Distances from each point in the catchment to the closest river reach are derived using GIS. An assumption made in the DDD model is that water moves to the closest stream network by waves with celerities related to the actual storage ($S(t)$) in the catchment (Skaugen & Mengistu, 2016). The hillslope distances combined with the celerity values are converted to the times needed to move water from each point in a catchment to the nearest river reach, called concentration times. The exponential distribution is found to be a good description of the cumulative distribution functions (CDF) of the distances to the closest stream (Skaugen & Onof, 2014). Hence, the exponential distribution can also be used to describe the distribution of concentration times. Skaugen and Onof (2014) used the CDF of concentration times to derive hillslope unit hydrographs (UH). The normal distribution was

found to fit well with the CDF of the distances from a point in the stream network to the outlet of a catchment. The river UH is determined from these river distances.

The capacity of the subsurface reservoir (*M*) in the DDD model is divided into five equal storage levels ($i$=1, …, 5) to estimate different celerity for different levels of saturation. The water starts filling the lowest storage level and increases to upper levels. The celerity for each storage level is estimated as described in the equation below

$$v_i = \frac{\lambda_i \, d_m}{\Delta t} \tag{2.6}$$

where $d_m$ is mean of the distances from hillslope points in the catchment to the closest river reach, and $\lambda_i$ is the UH$_i$ parameter for the storage level $i$. $\lambda_i$ is estimated such that the runoff from several storage levels will generate a hillslope UH that is equal to the exponential hillslope UH with a recession parameter $\Lambda_i$.

The saturated zone ($S(t)$) is calculated using the following equation

$$S(t) = \frac{Q(t)}{1 - e^{-\Lambda(t)}} \tag{2.7}$$

where $Q(t)$ is the released runoff and $\Lambda$ a parameter estimated through recession analysis. Details on estimation of $\Lambda$ are well described and can be found in (Skaugen & Mengistu, 2016; Skaugen & Onof, 2014).

The hillslope UHs are, as stated earlier, described by the exponential distribution. This is shown in the equation that follows

$$UH_i(t) = \lambda_i \, e^{-\lambda_i (t - t_0)} \tag{2.8}$$

where $t_0$ is the time of input and $\lambda_i$ is the exponential distribution parameter estimated for each storage level, $i$, through recession analysis. $\lambda_i$ has scale and recession parameters, named $Gscale$ and $Gshape$ respectively, derived from recession analysis of observed runoff. The distribution of the recession parameter ($\Lambda$) mentioned earlier can be modelled as a two-parameter gamma-distribution where $GscI$ and $GshI$ are scale and recession parameters, respectively (Skaugen & Mengistu, 2016).

The celerity of the river network (*rv*), a calibrated parameter in the DDD model, is considered in order to convert the stream network distance distribution into a distribution of travel times. This is used to derive the river network UH. The final convoluted UH is derived by combining the hillslope UHs and river UH as illustrated in Figure 2.1. The total runoff ($Q(t)$) generated from the catchment is estimated from the convoluted UH and excess water ($X(t)$).

### 2.5.4 Dynamic river network method

Like many other hydrological models, the DDD model is in many cases found to underestimate flood peaks. Tsegaw, Skaugen, et al. (2019) introduced a dynamic river network method into the DDD model to improve the flood peak estimation. They found that the flood peak prediction improved significantly when applying this method.

The DDD model has five storage levels, where four of them are subsurface level with limited capacity, and the fifth is an overland flow level with unlimited capacity (Skaugen & Mengistu, 2016; Skaugen & Onof, 2014). There are five UHs in total in the DDD model, four UHs for subsurface flow and one overland flow unit hydrograph (OUH). As different celerities are assigned to the different UHs, each UH has different temporal scales. When applying the dynamic river network routine in the DDD model, the four subsurface flow UHs remain constant while the scale of the OUH is dynamic during the simulation period (Tsegaw, Skaugen, et al., 2019). The shape of the travel time distribution in a hillslope is assumed constant, while the scale is assumed dynamic to generate dynamic OUHs. The dynamic OUHs in the DDD model are turned on and off depending on the saturation level of the subsurface. This gives a dynamic travel time distribution using the dynamic river network method.

Different assumptions considering parameters and the physical mechanisms have been made to derive the dynamic river network method (Tsegaw, Skaugen, et al., 2019). Three parameters, the mean ($D_m$) and maximum ($D_{max}$) of the hillslope distance distribution and the mean overland flow celerity ($v_{OF}$), must be computed in order to create the OUH. Tsegaw, Skaugen, et al. (2019) assumed that $v_{OF}$ is constant, the OUH is determined from $D_m$ and $v_{OF}$ exponentially, and that $D_m$ of a river network is a function of overland flow. Using the last assumption, a dynamic critical supporting area ($A_c$), which is the minimum drainage area required to initiate or maintain a river channel, can be derived. Firstly, the critical flux ($F_c$) must be determined as follows

$$F_c\left(m^3/_h\right) = A_c(m^2) * OF\left(m/_h\right) \tag{2.9}$$

where $OF$ is saturation excess overland flow. $OF$ is estimated at each simulation time step from the DDD model output. The value of $OF$ determines whether the dynamic river network routine is activated or not. When the subsurface is saturated and $OF > 0$, the dynamic river network routine is turned on and the corresponding $A_c$ is computed with Equation (2.9). The magnitude of $OF$ and $F_c$ controls contraction and expansion of the observed stream network. It is a general power relation between $D_m$ and $A_c$, shown in Equation (2.10), containing coefficients $a$ and $b$ that are computed for each catchment. $a$ and $b$ are estimated from a regression curve fitted to a relation between $D_m$ and $A_c$. The $A_c$ computed from Equation (2.9) is then used to estimate $D_m$ using Equation (2.10). When the $D_m$ computed with Equation (2.10) is bigger than the $D_m$ of the observed river network, the dynamic river network degenerates to the observed river network (Tsegaw, Skaugen, et al., 2019).

$$D_m = aA_c^b \quad (2.10)$$

### 2.5.5 DDD model parameters that require regionalisation

The DDD model is a parsimonious model with few calibration parameters. Most parameters are derived from catchment features. The model parameters that need regionalisation are estimated either by calibration or recession analysis of observed runoff, as presented in Table 2.1. In this study, the five calibration parameters ($PRO$, $Cx$, $CFR$, $Cea$, $rv$) are regionalised from 41 small catchments in Norway, which were calibrated by Tsegaw, Alfredsen, et al. (2019). The snow routine in DDD has three calibrated parameters that require regionalisation ($PRO$, $Cx$ and $CFR$). The snow routine also includes two non-regionalised parameters ($a0$ and $d$) for spatial distribution of snow water equivalent, a shape parameter ($a0$) and decorrelation length ($d$) respectively. The recession parameters ($Gscale, Gshape, GscI\ and\ GshI$) are estimated by recession analysis of observed runoff and the equations developed by Tsegaw, Alfredsen, et al. (2019), are used to in this study to estimate the recession parameters.

Table 2.1 DDD model parameters that need regionalisation.

| Parameter | Description | Unit | Method of estimation |
|---|---|---|---|
| PRO | Liquid water content in snow | % | Calibration |
| Cx | Degree day factor for snowmelt | mm/°C/h | Calibration |
| CFR | Degree day factor for refreeze | mm/°C/h | Calibration |
| Cea | Degree day factor for evapotranspiration | mm/°C/h | Calibration |
| rv | River flow celerity | m/s | Calibration |
| Gscale | Scale parameter of λ | Positive real number | Recession analysis of observed runoff |
| Gshape | Shape parameter of λ | Positive real number | Recession analysis of observed runoff |
| GscI | Scale parameter of Λ | Positive real number | Recession analysis of observed runoff |
| GshI | Shape parameter of Λ | Positive real number | Recession analysis of observed runoff |

## 2.6 Erosion processes

Erosion occurs in a river when more mass is removed than accumulated. Erosion, sedimentation, and transport and deposition of sediments are natural continuous processes in natural streams. Eroded masses are transported and deposited at new places downstream, which may change the flow pattern leading to erosion of other places in the stream. Most erosion occurs in the outer turns of streams where the water flows into the riverbank, and mass deposition and accumulation is most present in the inner turns (Jenssen & Tesaker, 2009). ). When the water velocity and force are high during flooding, the potential for erosion typically increases (Fergus et al., 2010).

It is important to be aware of common failure modes and erosion mechanisms when designing erosion control measures. The most common erosion mechanism is particle erosion. It is usually initiated by water flow, but ice can also contribute to particle erosion. Too small stone size, too

uniform stone gradation and too steep side slopes are probable causes of particle erosion (Brown & Clyde, 1989).

Stones are suitable materials for erosion protection. The size, density and shape of the stones are of great importance for channel stability. Cubic shaped stones, such as granite, gabbro and gneiss, that are resistant to frost and other loads are recommended for use in erosion control. The thickness of protection measures, the grading and compression of the particles and side slope also affect the channel stability (Jenssen & Tesaker, 2009).

### 2.6.1 Channel stability

Evaluation of channel stability is essential when designing erosion protection measures in a stream. Channel stability depends on the relationship between the average tractive force induced by the water flow and the river material's critical shear stress. The material is considered stable if the critical shear stress is greater than the tractive force. Observation is the best way to identify potential erosion of channel banks and hence the need for channel stabilisation (Brown & Clyde, 1989). Analytical methods for channel stability evaluation are, however, available.

Jenssen and Tesaker (2009) assessed different analytical methods for channel stability estimation, calculating stable stone size, based on shear either stress and water velocity. Shield's formula was recommended for stability estimations based on shear stress, and Maynord's method was recommended for calculations based on water velocity.

Maynord's formula is described Equation (2.11) and computes the size of a stable stone, *D30*, in the particular flow. $D_{30}$ is the characteristic stone size used in Maynord's method and describes the diameter of a stone with such a weight so that 30% of the other stones are of lighter weight.

$$D_{30} = S_f \, C_s \, C_V \, C_t \, y_0 \left[ \left( \frac{1}{s-1} \right)^{0.5} \frac{U}{\sqrt{K_1 g y_0}} \right]^{2.5} \tag{2.11}$$

where

$D_{30}$ = stable stone size (m)
$S_f$ = safety factor (-)
$C_s$ = stability coefficient (-)
$C_V$ = coefficient for vertical velocity distribution (-)
$C_t$ = coefficient for thickness of protection (-)
$y_0$ = water depth (m)
$s$ = specific density of stone (-)
$U$ = local water velocity (m/s)
$K_1$ = coefficient for side slope (-)
$g$ = gravitational acceleration (= 9.81 m/s$^2$)

Jenssen and Tesaker (2009) developed a graphical solution of Maynord's method with curves that is suitable for simple computations of stable stone size. This method comes with certain assumptions:

- Blasted rock with density, $p_s = 2600\ kg/m^3$
- Minimal thickness of protection layer, $t > 1.5\ D_{50}$ and $t > D_{max}$
- Longitudinal river slope $< 2\%$
- Safety factor, $S_f = 1$

*D30* is determined from Figure 2.2 if the assumptions above are fulfilled, and the side slopes are less steep than 1:4. For more details on Maynord's method, see Jenssen and Tesaker (2009).

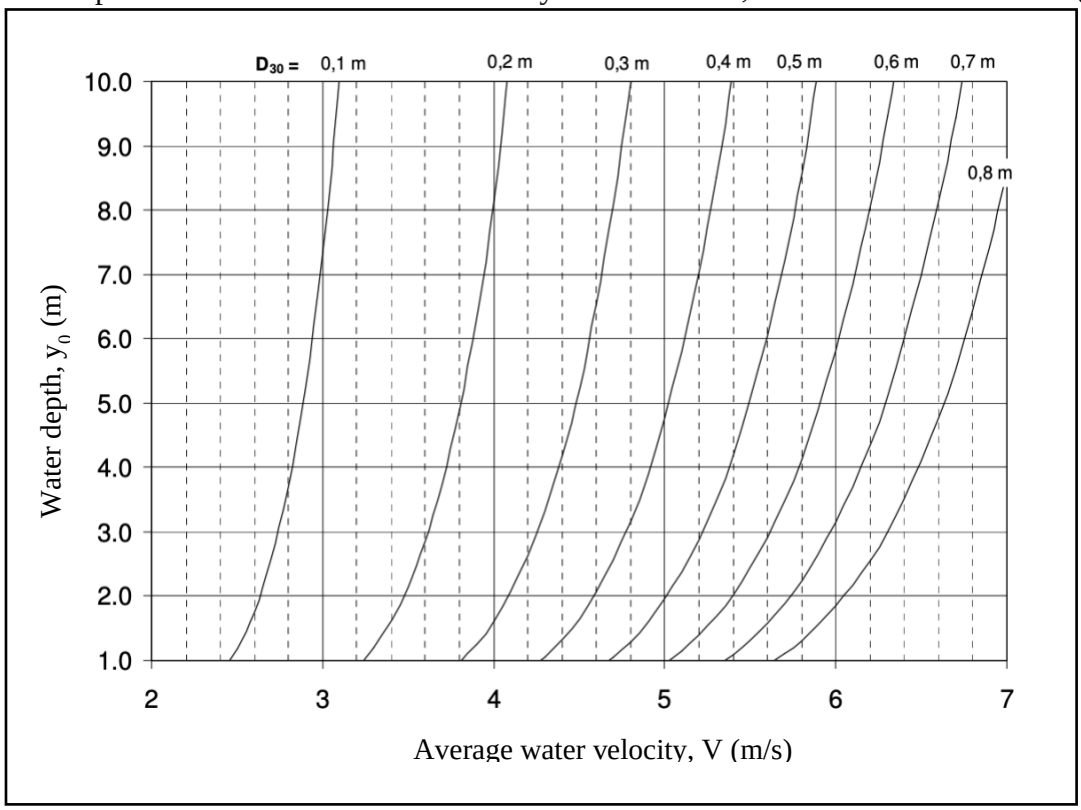


Figure 2.2 Curves for determination of *D30* as a function of water velocity and depth (Source: Jenssen and Tesaker (2009)).

# 3 Study area

Rv3 between Løten and Elverum located in Norway, is a part of a recently developed road that was opened in July 2020. The new road will improve the road connection between Oslo and Trondheim as Rv3 is the fastest and most important road between Oslo and Central Norway with a considerable number of heavy vehicles (NPRA, 2018b). Rv3 had annual average daily traffic (AADT) between 5000 and 6000 in 2020 at this section of the road (NPRA, n.d.). Hence, according to (NPRA, 2018a), the road is constructed for a flood with a 200-year return period (AADT > 4000).

A pilot project on stormwater management, in connection to parts of the new road, between Ommangsvollen and Grundset, and the surrounding catchment, is established by Klima2050. Klima2050 is a Norwegian Centre for Research-based Innovation that aims to reduce flood water exposure within the built environment and reduce the societal risks associated with climate change (Klima2050, n.d.-a). Skanska owns the pilot project, and the National Public Roads Administration (NPRA) and Multiconsult are participants. Parts of the objectives of the pilot project include documenting the functionality and efficiency of the installed stormwater management solutions and modelling surrounding catchments using the recently developed DDD modelling routine (Klima2050, n.d.-b).

A grassed swale is installed along a part of the new road as a stormwater management solution that should infiltrate, detain and convey stormwater from the road, and treat the road water before it is released into Stabekken. The infiltration swale is vegetated, and the swale surface, including the vegetation, is shown in Figure 3.1. However, detailed information on the vegetation and soil properties of the materials in the swale is not available.

Figure 3.1 Pictures of the swale surface and its vegetation (Photo by: Kristine Bergseng, 9th of November).

Instruments measuring outflow from the swale was planned in the downstream end of the swale. This is however not present, meaning outflow data, which is valuable for evaluation of the swale performance and calibration of the model, are not available.

During the process of establishing the new road, a part of Stabekken was rearranged. Stabekken is a nearby stream that previously crossed the area where the road now is located. To avoid Stabekken from crossing the new road, it was rearranged to be located along the road on the opposite side of the road from the studied swale, as shown in Figure 3.2 (left picture). A culvert is installed under the road draining water into Stabekken from the other side of the road. The culvert outlet in the rearranged part of Stabekken can be seen in Figure 3.2 (right picture).

Figure 3.2 The rearranged part of Stabekken, parts of the new road and the swale on the right side of the road during the construction period (left picture, Photo: Skanska). The rearranged part of Stabekken including the culvert outlet (right picture, Photo by: Mari Gilje Lillegraven, 9th of November).

The culvert was planned to drain the excess water from the swale into Stabekken. Hence the objective was to model and evaluate the effect of the road runoff from the swale on Stabekken. This should have been done by combining two models, a rainfall-runoff model of the swale and the flood estimation model of Stabekken. However, it was found that the culvert does not drain water from the swale as planned, but runoff from other areas such as agricultural land. Due to this, the objectives of the thesis were modified to model and evaluate the swale and rearranged part of Stabekken separately.

# 4 Method and Materials

This chapter describes the materials and methods used to address the objectives of the study. Description of the instrumental setup and the estimation of observed discharge in Stabekken, determination of design rain events that are used in modelling, how the swale and Stabekken are modelled using SWMM and the DDD model, respectively, and lastly, the approach used for estimating the channel stability in the stream, are included in this chapter.

## 4.1 Instrumental setup

Different instruments are installed at the study site to collect and record climate data, water level data in Stabekken and within the swale. The components of the instrumental setup are thoroughly described in the specialisation project (Lillegraven, 2020). A summarised description of the setup is given in the following sub-chapters, and illustrated in Figure 4.1.

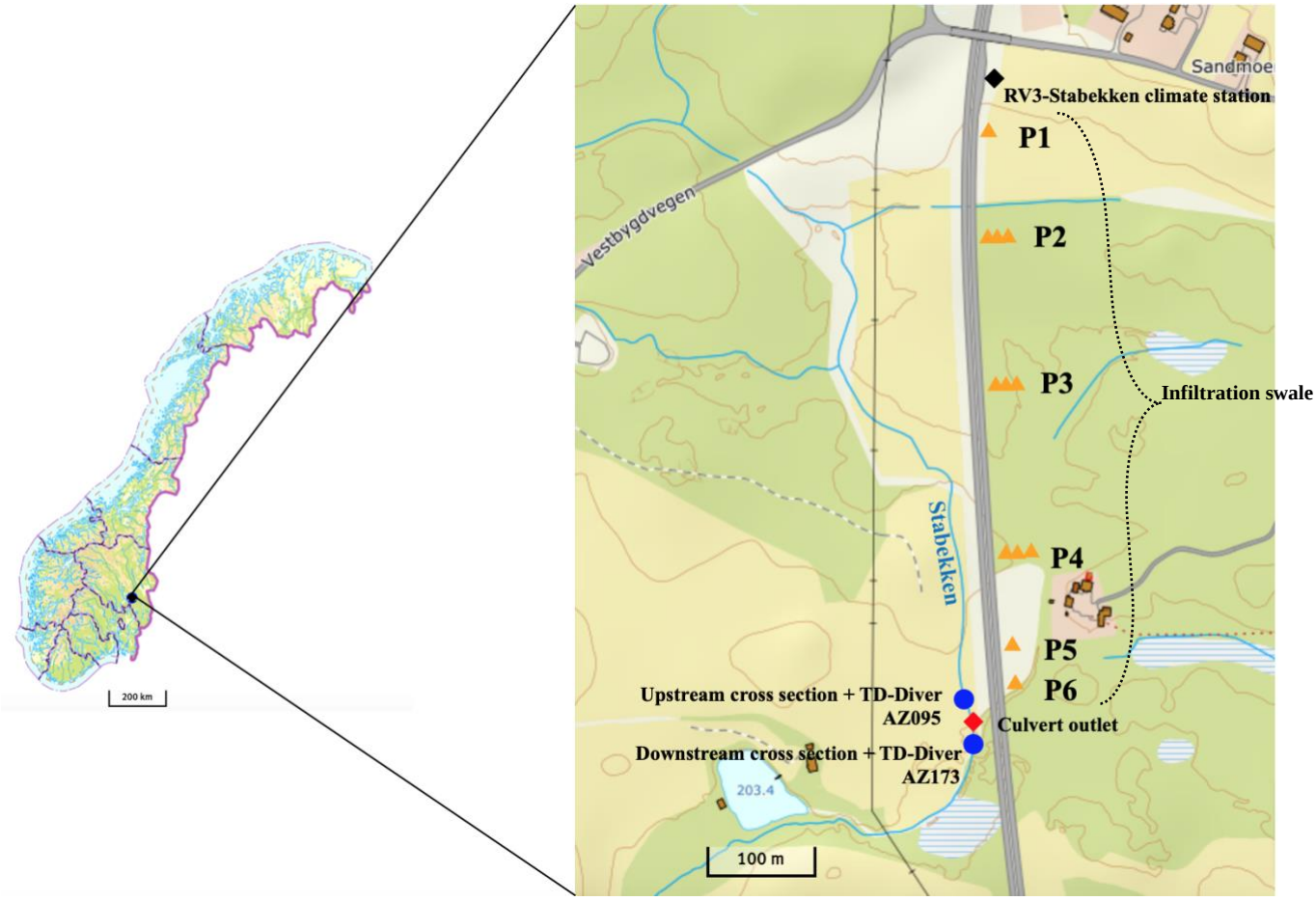


Figure 4.1 Overview and location of the study site and the installed instruments. Black square=Climate station, orange triangle=HOBO MX2001 Data Logger (the number of triangles at each position represents the number of sensor depths), red square=culvert outlet into Stabekken, blue circle=TD-Diver and GNSS measured cross section (Adapted from www.norgeskart.no).

A climate station owned by NPRA is installed upstream the swale. It includes among other instruments a laser disdrometer that records the type, amount and intensity of the precipitation as well as the kinetic energy and visibility. Temperature and precipitation data are collected from the climate station via NPRA's database.

12 copies of HOBO MX2001 Data Loggers are installed in the swale to record the water level at different depths and horizontal locations. The sensor depths are measured from the swale surface, and the water level above the sensor is measured, as illustrated in Figure 4.2. As illustrated in Figure 4.1, the water level data loggers are located at different sensor positions (P1, P2, P3, P4, P5 and P6) in the swale, and the number of vertical depths in each sensor position is illustrated with orange triangles. The time resolution of the data loggers is 10 minutes. The sensors are installed by NPRA to provide data that can contribute to the evaluation of the swale's performance.

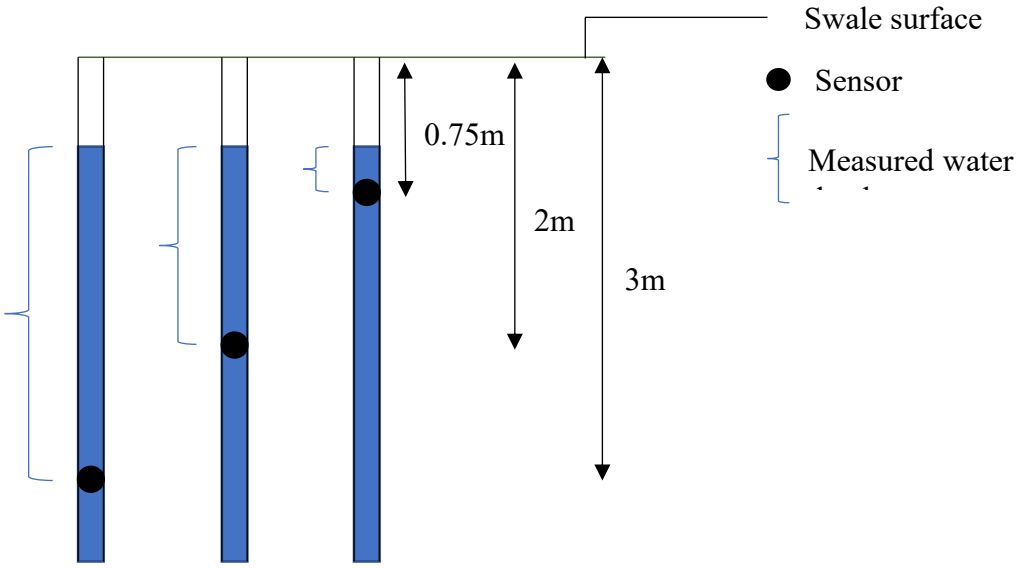


Figure 4.2 Illustration of how the water levels within the swale are measured.

Two cross sections of the rearranged part of Stabekken were measured using Global Navigation Satellite Systems (GNSS) instruments during fieldwork. The cross sections are located upstream and downstream the culvert outlet. A TD-Diver is installed at the river bed in each cross section. These divers measure the hydrostatic pressure. A Baro-Diver, which provide atmospheric pressure monitoring, is installed nearby Stabekken. The hydrostatic data is barometrically compensated and converted into water levels using the program Diver-Office.

### 4.1.1 Estimation of observed discharge

Manning's formula ($Q = \frac{1}{n} A R^{\frac{2}{3}} I^{0.5}$) is used to develop estimated stage-discharge curves in the upstream and downstream cross sections in Stabekken. Water level data measured with divers and GNSS-measured cross section geometry are used in the computations. Uniform flow is assumed when using Manning, which leads to uncertainties in the results. Limited data on the surface roughness is available. Hence Chow (1959), where typical n-values for various

channels are presented, is used when choosing the n-value for Stabekken. Based on this, $n = 0.05$ is chosen.

## 4.2 Determination of design precipitation events

Design precipitation events are used in the rainfall-runoff models to determine the magnitude of design floods for different return periods. Design precipitation events for specific durations and return periods are derived from Intensity-Duration-Frequency (IDF) curves. IDF curves represent the relationship between duration and intensity of precipitation, where the measure of frequency is the return period (O'Loughlin et al., 1996). The duration of the design precipitation events is assumed to be equal to the time of concentration (*tc*) of the catchment. *tc* is the time needed for water to flow from the farthest point in the catchment to the catchment outlet (Chow et al., 1998).

In this study, *tc* for Stabekken catchment is determined based on the method described in NPRA (2018a). The formula for $t_c$ is given for both undeveloped and developed areas, presented in Equations (4.1) and (4.2) respectively.

Undeveloped area: $$t_c = 0.6 * L * H^{-0.5} + 300 * Le \quad (4.1)$$

Developed area: $$t_c = 0.02 * L^{1.15} * H^{-0.39} \quad (4.2)$$

In the equations above, *tc* is the time of concentration (min), *L* is catchment length (m), *H* is elevation difference in the catchment (m) and *Le* is effective lake percentage (fraction). Hence, lakes in the catchment will dampen the flow in the catchment and delay response time in the catchment. This will not apply in Stabekken catchment as no lakes are present in the catchment. Stabekken is considered an undeveloped catchment, and thereby Equation (4.1) is used. The catchment characteristics used in the equation and their values, as well as *tc*, are presented Table 4.1

Table 4.1 The catchment characteristics (Effective lake percentage (*Le*), Catchment length (*L*), elevation difference in catchment (*H*)) used to calculate the time of concentration ($t_c$) in Stabekken catchment.

| Symbol | Description | Value | Unit |
|---|---|---|---|
| Le | Effective lake percentage | 0 | Fraction |
| L | Catchment length | 10500 | m |
| H | Elevation difference | 345 | m |
| $t_c$ | Time of concentration | 339.18 | min |

IDF curves are used to determine design precipitation events with a duration equal to *tc*. In this study, IDF curves are retrieved from the Norwegian Centre for Climate Services (https://klimaservicesenter.no/). This service provides IDF curves for durations between 1 minute and 24 hours with different return periods at any location in Norway. The uncertainty of data from the IDF curves increase with long return periods (Stenius et al., 2015). It is possible to choose any location and get IDF curves, also where a gauge station is not present. However, these IDF curves are based on gridded estimates and should not be used for accurate

dimensioning. There are only a limited number of gauges that provide exact IDF curves, and the closest station to Stabekken is located in Hamar, which is ca 10 km west of Stabekken. The local IDF curve from Stabekken and Hamar gauge with return periods 20 and 200 years and durations 0 – 360 minutes are presented in Figure 4.3. The local curves are the most conservative. Hence, the local IDF curves from Stabekken are used for further computations of design events.

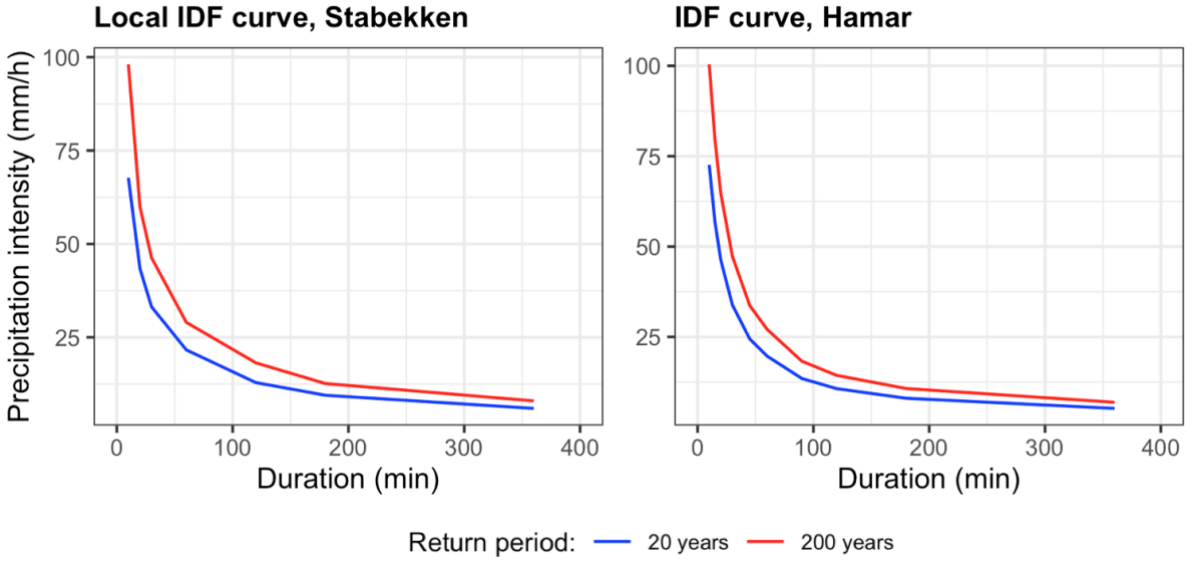


Figure 4.3 IDF curves for 20- and 200-year return periods for Stabekken based on gridded estimates and Hamar gauge (adapted from https://klimaservicesenter.no/).

The climate is changing, and extreme rainfall events will increase in size and frequency in the future. Hence, a 40% climate factor is added to the precipitation in the IDF curves to account for this increase (Dyrrdal & Førland, 2019). IDF curves for Stabekken including a 40% climate factor with return periods of 20 and 200 years are presented in Figure 4.4.

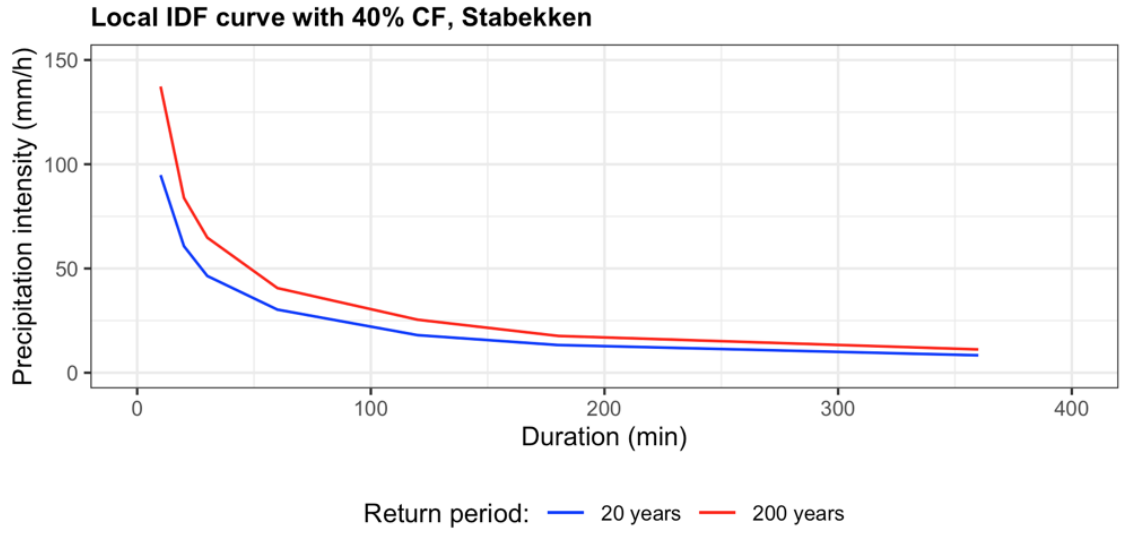


Figure 4.4 IDF curves for 20- and 200-year return periods for Stabekken based on gridded estimates used to create symmetrical hyetograph which is used in the SWMM model as design rain events (adapted from https://klimaservicesenter.no/).

Symmetrical design hyetographs, with and without 40% climate factor, are computed using the procedure described in Ødegaard (2014), and used when modelling the swale runoff and floods in Stabekken to simulate effects of extreme rainfall events in the systems. Design events with 20- and 200-years return periods are computed for use in the swale modelling, as presented in Figure 4.5. The hyetographs used when modelling the swale have 5-minute time steps and durations of 60 minutes. This is due to the lack of known *tc* for the catchment that drains into the swale. For Stabekken, the duration of design events is set to $360\,\text{min} \approx t_c$. The time steps in the hyetograph used when modelling Stabekken is set to 60 minutes since the DDD model has hourly time resolution. Design events when estimating flood peaks in Stabekken, with 200-year return period, are presented in Figure 4.6.

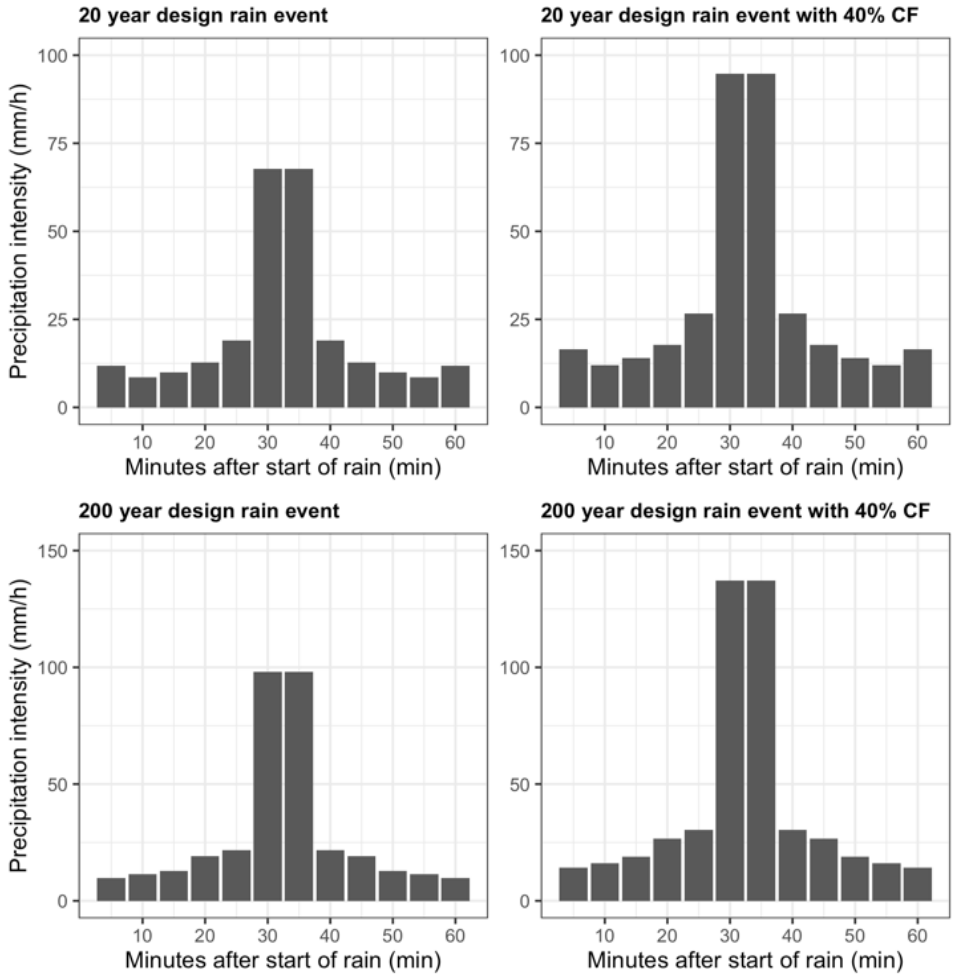


Figure 4.5 Design precipitation events used modelling swale runoff in SWMM given in (mm/h).

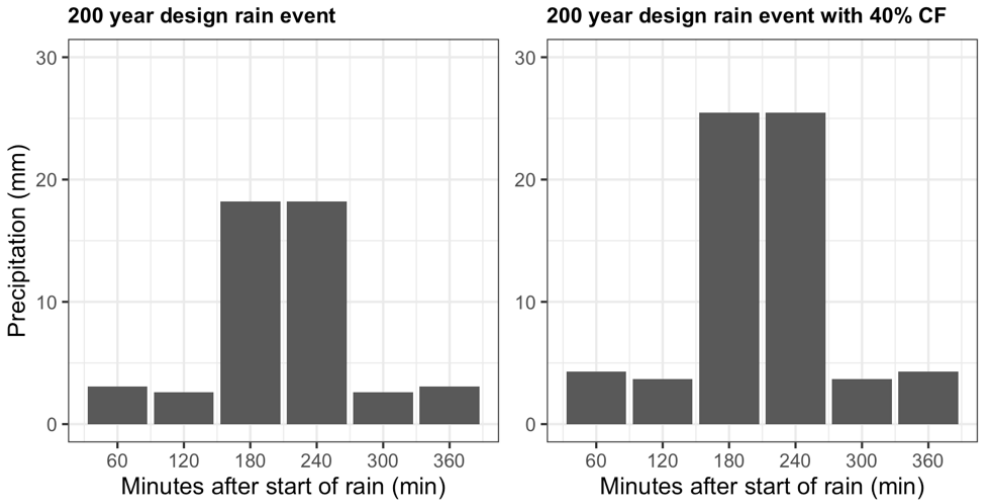


Figure 4.6 Design precipitation events used for flood peak modelling in Stabekken. Precipitation input in the DDD model is given in volume, hence the design events are given in volume (mm).

Design precipitation events are used in the models to simulate runoff and flow during extreme rain events. For the DDD model, which is a continuous model, the design events are added at different catchment conditions. The saturation level of the catchment and the water level in Stabekken at the start of the design precipitation event affects the magnitude of the generated flood. Dry and wet conditions and during snowmelt are set as antecedent soil moisture conditions at the start of the design events. These conditions are identified by running the DDD model without the design precipitation events. Dry conditions are determined by identifying long periods of little precipitation and low discharge values in Stabekken, typically during summer. Wet conditions are identified by periods of precipitation and high discharge values, typically found during spring or autumn. Periods of snowmelt are identified by studying the simulated snow storage in the catchment.

## 4.3 Modelling the swale using SWMM

SWMM is used to model the water transport in the infiltration grass swale installed along Rv3. A brief description of SWMM is given in Chapter 2.4.1. The following describes how the rainfall-runoff model of the swale is set up using SWMM.

The model is set up of subcatchments that receive precipitation from a rain gauge and generate runoff. The road is the area that drains into the swale. This road area is divided into five subcatchments. The swale is also divided into five subcatchments. Hence, one road subcatchment drains into one swale subcatchment, and each swale subcatchment drains into the swale subcatchment downstream. Each road subcatchment has an area of 580 $m^2$, and each swale subcatchment has an area of 1111 $m^2$. The most downstream swale subcatchment drains into an outfall node. The total drainage area of the outfall node is 8455 $m^2$. Figure 4.7 presents the graphical model setup. The reason for dividing the road and swale areas into five subcatchments is to distribute the precipitation and runoff input over the length of the road and the swale. A subcatchment can only have a single inflow and outflow point, hence dividing the areas is appropriate. A LID control defined as a vegetative swale is assigned to occupy the total area of each swale subcatchment.

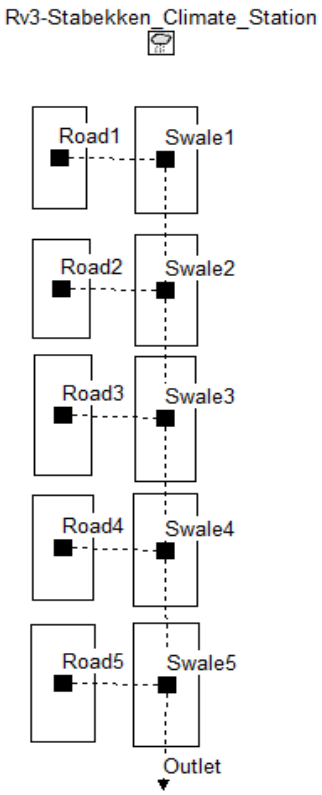


Figure 4.7 The model setup in SWMM of the swale and its draining subcatchments at Rv3. The model setup of the swale and its draining subcatchments at Rv3. The left rectangles represent the road and swale areas, respectively. The cloud on top represents the rain gauge, and the triangle at the bottom represents the outfall node.

Both a long-term precipitation simulation and single-event based simulations are conducted. The continuous long-term simulation uses a precipitation time series covering the same period as the measured water level data within the swale. The water level data are analysed and used to choose infiltration parameters so that the model simulates the same runoff as the measurements show during the monitoring period. Suppose the measurement data analysis show no runoff from the swale during the period. In that case, the infiltration parameters in the model should be modified (e.g. decrease hydraulic conductivity) such that no runoff is produced in the model. This is done to optimise the model since no data on the infiltration capacity of the built swale is given. The modified model is used when running single-event simulations. Design precipitation events of 20- and 200-years return periods derived from IDF curves from Stabekken are used in the single-event simulations in SWMM. The duration of the events are 60 minutes, and the return period of the design event are 20 and 200 years. A return period of 200 years is used due to the guidelines given by NPRA (2020) based on the safety class of the road. A return period of 20 years is used in SWMM simulations to give a perspective on the swale runoff expected to occur on average one time during 20 years.

### 4.3.1 SWMM parameters

SWMM requires different parameters for the subcatchments and the LID control. The chosen values as well as a description of the parameters required for the vegetative swale (LID-control) are presented in

Table 4.2 (Rossman, 2015). They were obtained using literature, SWMM default values and available data on the physical properties of the swale.

Table 4.2 Parameters required for the vegetative swale in SWMM, parameter descriptions, chosen values.

| Parameter | Description | Value | Source |
|---|---|---|---|
| Berm height (mm) | The maximum depth above the surface of the vegetative swale before overflow occurs, i.e. the height of the trapezoidal cross section. | 880 mm | Available geometry data on the swale |
| Vegetation volume (fraction, 0-1) | Volume of the storage depth filled with vegetation, not the vegetation surface coverage. | 0 | Default SWMM value |
| Surface roughness (Manning's n) | Manning's n for flow over the swale surface. | 0.04 (M=25) | (NPRA, 2018a) (Rossman, 2015) |
| Surface slope (%) | The longitudinal slope of the swale. | 0.5 | Available geometry data on the swale and (NPRA, 2018a) |
| Swale side slope (run/rise) | The side wall slope of the swale's cross section. | 2 | Available geometry data |

Evaporation, which is included in climatology, is neglected when running event-based simulations. During the continuous long-term precipitation simulation, monthly evaporation rates for southern Norway are used (Engeland et al., 2004).

Green-Ampt is chosen as the infiltration method. The chosen infiltration parameter values are based on literature (Rossman, 2015, 2016), and the modifications conducted in the long-term precipitation simulation based on the water level measurements within the swale.

When running the SWMM model, it is essential to set the simulation period similar to the period of the input time series, and the time interval of the rain gauge identical to the time interval of the data in the input time series.

## 4.4 Flood prediction in Stabekken (DDD model) – Data extraction and processing

The DDD model is used to estimate flow in Stabekken. The structure of the model is described thoroughly in sub-chapter 2.5. The DDD model is written in the programming language R. The input files to the model are one file containing the parameter values of the model (parameter file) and another file containing precipitation and temperature for each elevation zone in the catchment (PTQ-file). The dynamic river network routine is included in this study due to the recommendations by Tsegaw, Skaugen, et al. (2019). The dynamic river coefficients *a* and *b* are put in separately in the model.

### 4.4.1 Precipitation and temperature data

Gridded hourly precipitation and temperature data from the seNorge2 database are used in this project (MET, n.d.). The data are produced in grid formats with 1x1km sized grids (Lussana et al., 2018). The datasets are provided by the Norwegian Meteorological Institute (MET). Hourly gridded precipitation and temperature data are available from 2010 to the current date. In this study, data from January 2018 to May 2021 distributed across the 10 elevation zones of the catchment are used as input to the DDD model. Different scripts are used to prepare the temperature and precipitation input distributed across the 10 elevation zones of the catchment. A python script is used to download gridded hourly precipitation and temperature data as NetCDF files from seNorge2. One NetCDF file contains one hour of either gridded precipitation or temperature data. The coordinates of the grid points within Stabekken catchment and their assigned precipitation and temperature value are extracted using an R script that uses the downloaded NetCDF files as input. Another R script uses the coordinates of the grid points and the catchment DEM to assign the grid points and their respective climate data to the different elevation zones. The output of this script is the PTQ-file which is one of theinput files in the DDD model. The 10 elevation zones and location of gridded input (temperature and precipitation) in Stabekken is shown in Figure 4.8.

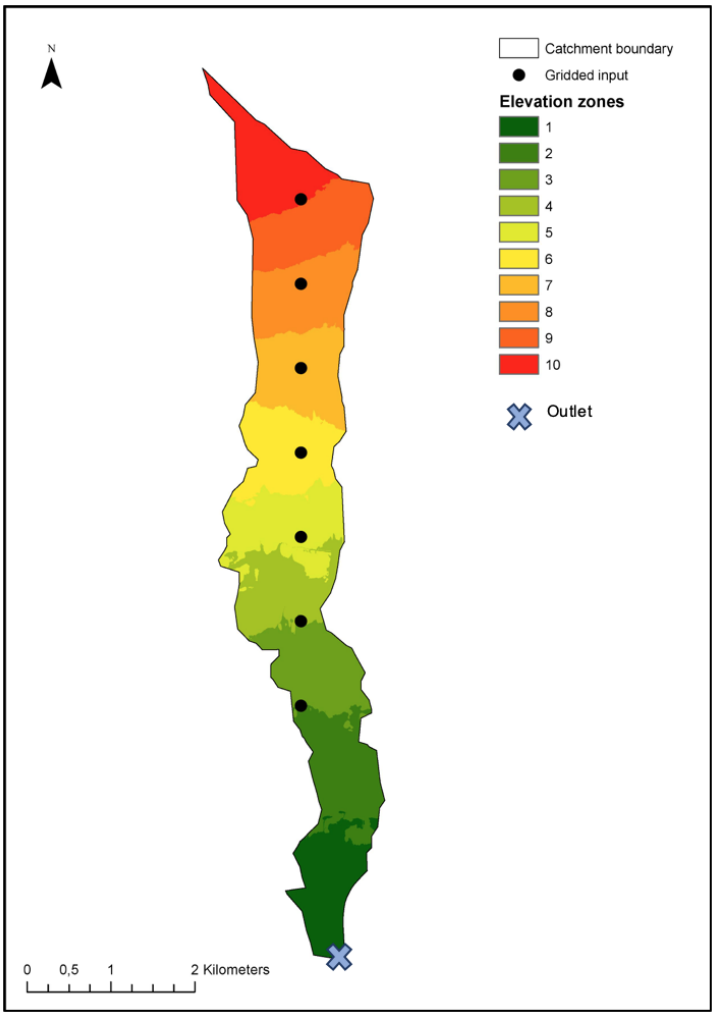


Figure 4.8 Elevation zones, and gridded climatic input (temperature and precipitation) in Stabekken catchment.

### 4.4.2 Catchment descriptors extraction

NEVINA and ArcMap are used to extract catchment descriptors (CDs) from Stabekken catchment. These CDs create the parameter file that is input in the DDD model. NEVINA, an online tool (http://nevina.nve.no) owned by the Norwegian Water and Energy Directorate (NVE), is used to delineate catchments and extract catchment information. A drainage point located in or near a defined river network is needed to generate a catchment. For Stabekken catchment, the drainage point was located downstream the culvert outlet, and some editing was done to exclude the water draining from the road to the swale. The extracted catchment delineation and information is shown in Figure 4.9. ArcMap version 10.8.1 is a GIS program that, in this study, is used to create maps and extract CDs for further use in modelling discharge in Stabekken. Table 4.3 shows the parameters obtained from geographical and hydro-meteorological data from the catchment and the tools used to extract the different parameters.

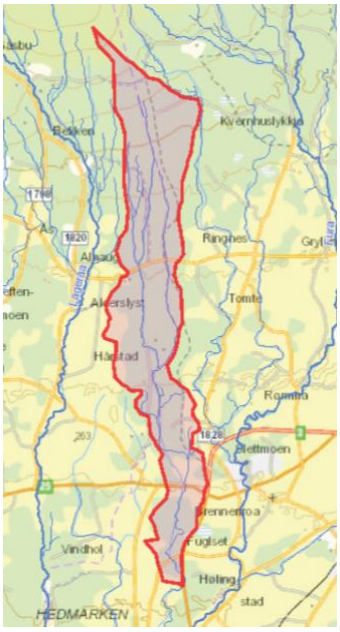


| Feltparametere | | |
|---|---|---|
| Areal (A) | 10.1 | km² |
| Effektiv sjø ($A_{SE}$) | 0 | % |
| Elvleengde ($E_L$) | 10.9 | km |
| Elvegradient ($E_G$) | 22.3 | m/km |
| Elvegradient$_{1085}$ ($E_{G,1085}$) | 18.7 | m/km |
| Helning | 1.9 | ° |
| Dreneringstetthet ($D_T$) | 2.2 | km$^{-1}$ |
| Feltlengde ($F_L$) | 10.5 | km |

| Arealklasse | | |
|---|---|---|
| Bre ($A_{BRE}$) | 0 | % |
| Dyrket mark ($A_{JORD}$) | 11.3 | % |
| Myr ($A_{MYR}$) | 0.5 | % |
| Leire ($A_{LEIRE}$) | 0 | % |
| Skog ($A_{SKOG}$) | 86.0 | % |
| Sjø ($A_{SJO}$) | 0.0 | % |
| Snaufjell ($A_{SF}$) | 0 | % |
| Urban ($A_U$) | 0.4 | % |
| Uklassifisert areal ($A_{REST}$) | 1.7 | % |

| Hypsografisk kurve | | |
|---|---|---|
| Høyde$_{MIN}$ | 204 | m |
| Høyde$_{10}$ | 234 | m |
| Høyde$_{20}$ | 261 | m |
| Høyde$_{30}$ | 284 | m |
| Høyde$_{40}$ | 299 | m |
| Høyde$_{50}$ | 313 | m |
| Høyde$_{60}$ | 334 | m |
| Høyde$_{70}$ | 360 | m |
| Høyde$_{80}$ | 393 | m |
| Høyde$_{90}$ | 424 | m |
| Høyde$_{MAX}$ | 549 | m |

| Klima- /hydrologiske parametere | | |
|---|---|---|
| Avrenning 1961-90 ($Q_N$) | 7.4 | l/s*km² |
| Sommernedbør | 346 | mm |
| Vinternedbør | 285 | mm |
| Årstemperatur | 2.3 | °C |
| Sommertemperatur | 11.1 | °C |
| Vintertemperatur | -3.9 | °C |

Figure 4.9 NEVINA outputs, catchment delineation and information, from Stabekken catchment. (Source: http://nevina.nve.no/).

Table 4.3 Catchment descriptors and model parameter for the DDD model derived from NEVINA and ArcMap.

| Category | CD | Description | Unit | Source |
|---|---|---|---|---|
| Topographic data | Area | Catchment area | km$^2$ | NEVINA |
| | Me | Mean elevation (DTM10) | m | ArcMap |
| | RL | River length | km | NEVINA |
| | Rs | River slope | m/km | NEVINA |
| | HC | Hypsographic curve | - | NEVINA |
| Hydro-meteorological data | Mp | Mean annual precipitation | mm/year | NEVINA |
| | Mt | Mean annual temperature | °C/year | NEVINA |
| | Sq | Specific runoff | l/s/km$^2$ | NEVINA |
| Land cover data | G | Glacial cover | % | NEVINA |
| | CL | Cultivated land | % | NEVINA |

| | | | | |
|---|---|---|---|---|
| | M | Marsh land | % | NEVINA |
| | C | Clay land | % | NEVINA |
| | F | Forest cover | % | NEVINA |
| | B | Bare mountain | % | NEVINA |
| | U | Urban land | % | NEVINA |
| | UA | Unclassified area | % | NEVINA |
| | La | Lake | % | NEVINA |
| | Le | Effective lake | % | NEVINA |
| River length from the outlet | midFL | Mean | m | ArcMap |
| | stdFL | Standard deviation | - | ArcMap |
| | maxFL | Maximum | m | ArcMap |
| Marsh land distance to river networks | midLbog | Mean | m | ArcMap |
| | stdbog | Standard deviation | - | ArcMap |
| | maxLbog | Maximum | m | ArcMap |
| | Zbog | Zero fraction | - | ArcMap |
| Soil distance to river networks | midDL | Mean | m | ArcMap |
| | stdDL | Standard deviation | - | ArcMap |
| | maxDL | Maximum | m | ArcMap |
| | Zsoil | Zero fraction | - | ArcMap |
| Glacier distance to river networks | midGL | Mean | m | ArcMap |
| | stdGL | Standard deviation | - | ArcMap |
| | maxGL | Maximum | m | ArcMap |

ArcMap is used to extract CDs and model parameters for the DDD model. All layers created in ArcMap are saved to a created geo database. The preparation in ArcMap for further CDs extraction is described below:

1. Download shapefile of the catchment from NEVINA as previously described and add the layer into ArcMap.
2. Download DTM 10x10m from the Norwegian Mapping Authority (https://hoydedata.no/LaserInnsyn/) and add the layer into ArcMap.
3. “Mosaic to new raster” is used to merge two DTM rasters to cover the catchment. This step depends on the spatial coverage of the DTM.
4. “Clip” under “Data management tools” raster with shapefile of the catchment from NEVINA to clip the DTM, so it fits the shape of the catchment.
5. Download observed stream networks from NVE (https://temakart.nve.no/tema/elvenett) and add the layer into ArcMap.
6. Use the “Editor” toolbar to merge the stream network into one polyline. The tool “merge” is used for this.
7. “Clip” stream network with respect to the catchment.
8. “Polyline to raster” is used to convert the observed stream network from a polyline feature to a raster dataset.

Steps to obtain values for river lengths to the outlet:

The following procedures are applied in ArcMap to obtain the statistics of the river distances from the outlet, river lengths to the outlet of the catchment, and are illustrated inFigure 4.11:

1. “DEM Reconditioning” found under “Terrain Preprocessing” in the ArcHydro toolbox is used to modify the DTM10 to fit the observed stream network in the catchment.
2. “Fill” under “Hydrology toolbox” is used with the modified DTM10 as input to fill sinks with an undefined drainage direction where no surrounding cells have lower elevation.
3. “Flow direction” under “Hydrology toolbox” is used to determine the direction of flow from cell to cell. The eight-direction pour point (D8) method is used. Each cell is assigned flow to one of its eight neighbours in the direction with the steepest downhill slope, either adjacent or diagonal. The flow direction encoding in ArcMap is illustrated in Figure 4.10. The filled modified DTM10 is the input raster.
4. “Flow length” under “Hydrology toolbox” is used to determine the distance from each cell to the outlet in the catchment. The flow direction map is used as input.
5. “Extract by mask” under “Spatial analyst” toolbox extract the distances of the stream network to the outlet. The flow length raster and the stream network raster are inputs.
6. “Zonal statistics as table” is then used to obtain the distance distribution statistics (mean, maximum and standard deviation) from each cell of the stream network to the outlet. The stream network raster and the extracted distances are used as inputs.

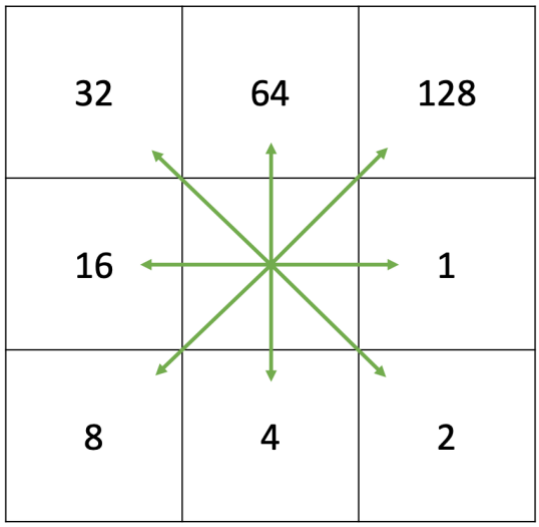


Figure 4.10 The flow direction encoding (eight-direction pour point (D8) method) used in ArcMap.

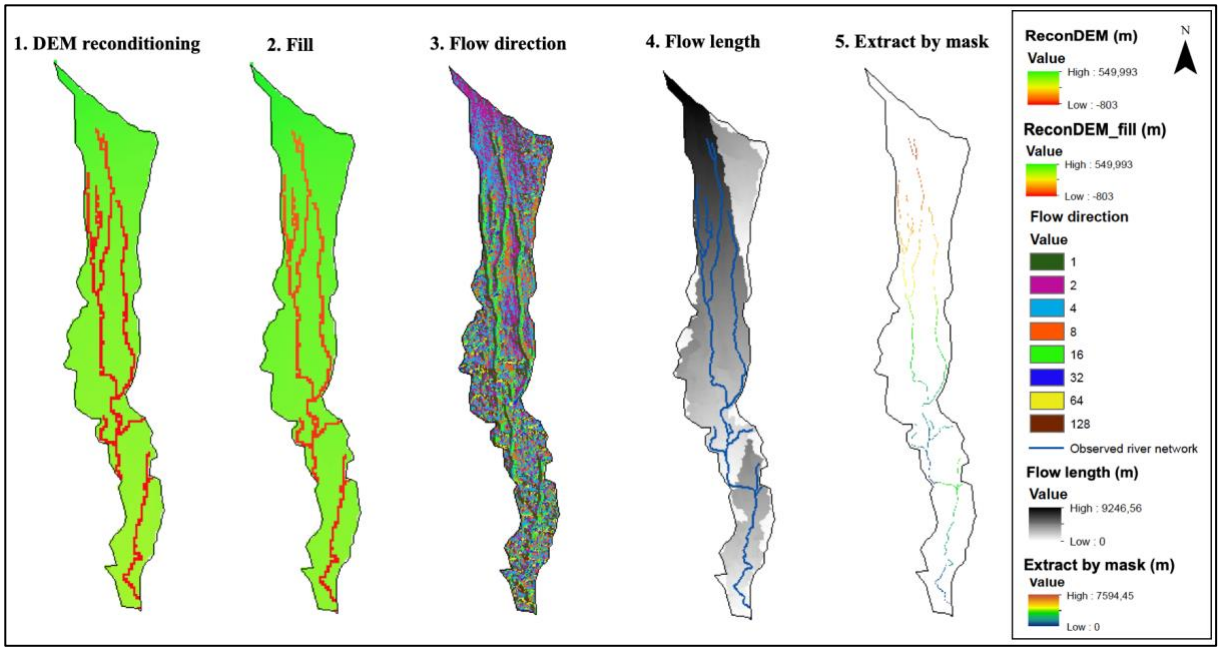


Figure 4.11 Steps to obtain river distances from the outlet for Stabekken catchment, using ArcMap.

Statistics of distances of marsh land, non-marsh land and glacial cover to river networks:

The Euclidean distances, which is the shortest length of a straight line between two points, to the river network in the catchment for each land cover type are obtained applying the following steps in ArcMap:

1. Download land cover types data, AR50, from www.nibio.no, a service owned by the Norwegian Institute of Bio-Economic Research. Download as a shapefile, convert to raster with "Polygon to raster".
2. "Reclassify" is used to reclassify the land cover types data to marsh land, non-marsh land and glacier lands. The land cover raster is used as input. The reclassified land cover types and the observed stream network in Stabekken catchment are shown in Figure 4.12.
3. "Euclidean distance" determines the Euclidean distances from the observed stream network. The stream network raster is used as input.
4. "Zonal statistics as table" is used to determine the distance distribution statistics (mean, maximum and standard deviation) for each reclassified land cover type. The reclassified land cover raster and the Euclidean distances are used as inputs.
5. "Extract by mask" is used to extract the distances from the different land cover types to the stream network. The reclassified land cover and the stream network raster are used as inputs.
6. "Zonal geometry as table" is used to determine the amount of area of each reclassified land cover type that has zero distance to the stream network. The extracted distances from each land cover to the stream network are used as inputs. The zero fractions of the different land covers (*Zbog* and *Zsoil*) are determined by dividing the zero distance areas by the total area of the land cover types.

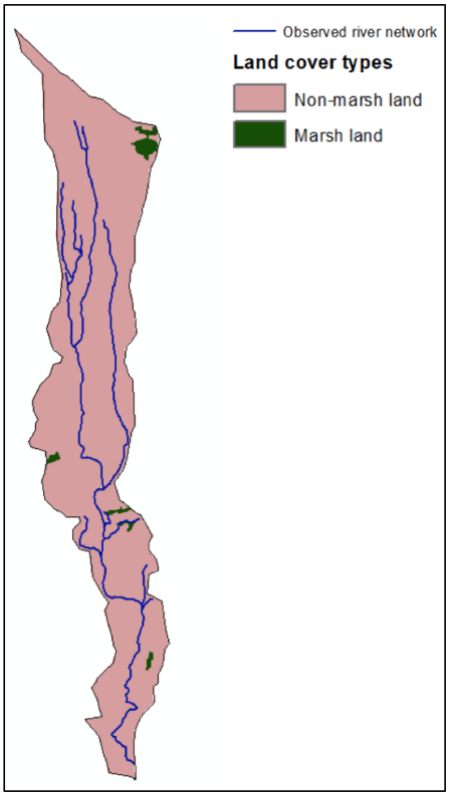


Figure 4.12 Observed river network and land cover types in Stabekken catchment (Adapted from ArcMap).

### 4.4.3 Determination of dynamic river network coefficients

The coefficients *a* and *b* of the relation between the mean of the hillslope distance distribution (*Dm*) and critical source area (*Ac*) (Equation (2.8)) must be computed to account for the dynamic river network routine in the DDD model. The following procedure is used to determine *a* and *b* (all previous steps in ArcMap described earlier should be conducted first):

1. "Flow accumulation" under "Hydrology toolbox" is used to create a raster of accumulated flow into each cell. The flow direction map is used as input.
2. Create a shapefile only including the non-marsh lands. This is done by erasing the cells, including marsh land and glacier land. "Greater than" and "Set null" under "Spatial analyst tools" are used to conduct this. The reclassified raster, including the land cover types, is used as input.
3. A separate python script is used to loop through different thresholds of critical source areas (*Ac*) from the flow accumulation to define and create different stream networks. A separate python script is used to create several stream networks by looping through different thresholds of critical source areas (*Ac*) from the flow accumulation. The *Dm* is calculated for each stream network. The flow accumulation raster and the shapefile, including the non-marsh lands, are inputs in the python script.
4. A separate R script is used to fit a regression curve to the synthetically determined values for *Dm* and *Ac*. The coefficients *a* and *b* are derived, and these are unique for Stabekken catchment. The curve fitted to the relation between *Dm* and *Ac* ($D_m = aA_c^b$), and the *a* and *b* values, as well as the correlation coefficient *R2* for Stabekken catchment, are shown in Figure 4.13.

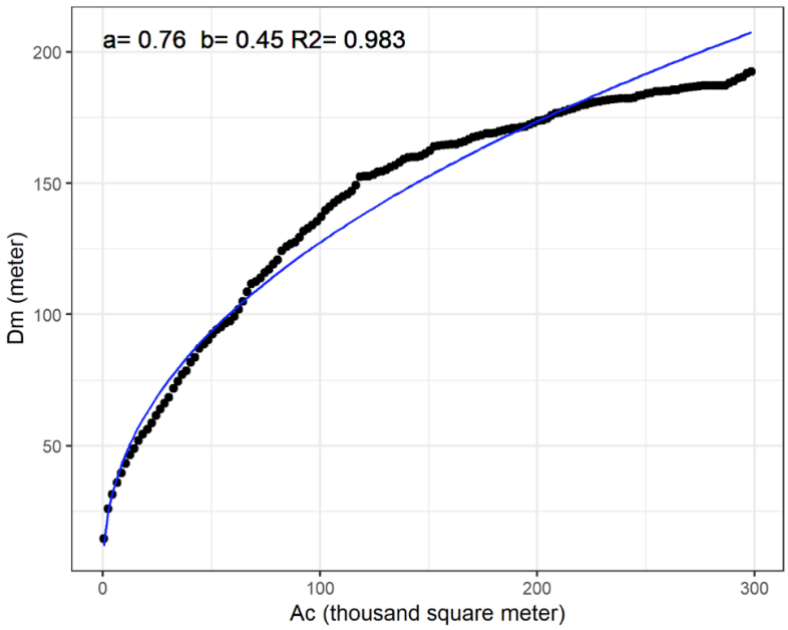


Figure 4.13 Regression curve fitted to the relation between the mean of the hillslope distance distribution (*Dm*) and the critical source area (*Ac*) ($D_m = aA_c^b$), and the values of coefficients *a* and *b*, and the correlation coefficient $R^2$.

## 4.5 Regionalisation methods for estimation of DDD model parameters

Stabekken catchment is a small ungauged catchment that requires regionalisation for estimation of model parameters. Physical similarity, spatial proximity and regression, three of the most common regionalisation methods, are described in chapter 2.3. Tsegaw, Alfredsen, et al. (2019) found in their study on hourly flow estimation with the DDD model in ungauged catchments that a combined regionalisation method performed best. The combined method includes the multiple regression method and physical similarity method. The multiple regression method estimates the recession parameters (*Gscale, Gshape, GscI* and *GshI*). The pooling group method of physical similarity estimates the calibration parameters in the DDD model (*PRO, Cs, CFR, Cea* and *rv*).

### 4.5.1 Regression method

For the regression method, empirical relationships, including catchment descriptors from the ungauged catchment, estimate the recession parameters. Tsegaw, Alfredsen, et al. (2019) developed regression equations during their study on hourly flow estimation in small ungauged catchments using the DDD model. These equations are used in this study on flow estimation in Stabekken and are presented in Equations (4.3) – (4.7). The recession parameters (*Gscale, Gshape, GscI* and *GshI*) are estimated using multiple regression, and the critical flux (*Fc*) is estimated with single regression.

$$Gscale = \exp\left(-5.12 - 0.12 * L_e + 0.22 * \ln(S_q) + 0.3 * \log(M_e)\right) \quad (4.3)$$

$$Gshape = 0.82 + 0.0005 * M_p - 0.009 * S_q \quad (4.4)$$

$$GscI = 0.49 * Gscale - 0.0014 \quad (4.5)$$

$$GshI = 2.047 * Gshape - 0.658 \quad (4.6)$$

$$F_c = 160.7 - 1.4 * \mathrm{B} \quad (4.7)$$

The catchment descriptors used in the empirical regression equations presented above are effective lake percentage ($L_e$), specific runoff ($S_q$), mean elevation ($M_e$), mean annual precipitation ($M_p$) and bare mountain percentage (B). Values of these catchment descriptors are presented in Table 4.5. The results estimated using regression are presented in Table 4.4.

Table 4.4 DDD model parameters estimated using regression.

| Parameter | Value | Unit |
|---|---|---|
| Gscale | 0.0197 | - |
| Gshape | 1.069 | - |
| GscI | 0.00824 | - |
| GshI | 1.530 | - |
| Fc | 160.7 | $m^3/h$ |

## 4.5.2 Physical similarity method

As described in sub-chapter 2.3.1, parameter sets are transferred from similar gauged catchments to the ungauged catchment in the physical similarity method. In this study, similarity is assessed using the similarity index (*SI*). 12 CDs are used to perform the physical similarity assessment. These CDs and their value in Stabekken are presented in Table 4.5.

Table 4.5 Catchment descriptors used in the regression equations and the similarity assessment.

| Symbol | Description | Value (Stabekken) | Unit | Source |
|---|---|---|---|---|
| A | Catchment area | 10.09 | $km^2$ | NEVINA |
| midFL | Mean of river length from outlet | 3526.49 | m | ArcMap |
| midLbog | Mean of marsh land distance to river | 530.36 | m | ArcMap |
| midDL | Mean of non-marsh land distance to river | 150.04 | m | ArcMap |
| Le | Effective lake percentage | 0 | % | NEVINA |
| F | Forest percentage | 86.01 | % | NEVINA |
| B | Bare mountain percentage | 0 | % | NEVINA |
| U | Urban percentage | 0.44 | % | NEVINA |
| Me | Mean elevation | 317.91 | m | ArcMap |
| Mp | Mean annual precipitation | 631 | mm/year | NEVINA |
| Sq | Specific discharge | 7.4 | $l/s/km^2$ | NEVINA |
| Rs | River slope | 18.7 | m/km | NEVINA |

In this study, *SI* is computed for 41 gauged catchments calibrated by Tsegaw, Alfredsen, et al. (2019) using the DDD model. Table **4.6** shows the catchments that produce the lowest *SI* with

Stabekken and their values. Fura catchment generates the smallest *SI*, indicating that Fura is the most physically similar gauged catchment to Stabekken catchment among the 41 calibrated catchments investigated. Fura is in addition located close by Stabekken. Hence Fura is used as a single donor in this study.

Table 4.6 Seven of the 41 calibrated catchment with smallest similarity indexes (*SI*) with respect to Stabekken catchment.

| Station name | Station ID | Similarity Index (SI) |
|---|---|---|
| Fura | 2.323 | 3.63 |
| Gryta | 6.1 | 4.63 |
| Sæternbekken | 8.6 | 4.84 |
| Hangtjern | 12.212 | 4.00 |
| Grosettjern | 16.66 | 4.97 |
| Rekedalselv | 26.64 | 5.06 |
| Svarttjørnbekken | 123.29 | 4.21 |

In this study, two different parameter sets are tested when modelling the flow in Stabekken. The first parameter set used is determined using the combined method described by Tsegaw, Alfredsen, et al. (2019). Here, regression equations (4.3 – 4.7) are used to estimate the recession parameters (*Gscale, Gshape, GscI* and *GshI*). The calibration parameters from the snow routine (*PRO, Cx, CFR, Cea, rv*) are transferred from Fura which is found to be the most similar gauged catchment to Stabekken. In the other parameter set that is tested when estimating flow in Stabekken, both recession and calibration parameters are directly transferred from Fura. The shape parameter (*a0*) and decorrelation length (*d*) of the snow water equivalent and gamma snow distribution are also transferred directly from Fura. These two different model parameter sets are used when modelling Stabekken to investigate the difference in model results depending on the parameters chosen. Fura's parameter set is presented in Table 4.7.

All parameters used for flow estimation in Stabekken are summarised in the parameter files presented in Appendix D (Table **0.1** and Table **0.2**). A parameter file is one of two input files to the DDD model.

Table 4.7 Model parameters from Fura catchment which is used as a single donor for Stabekken.

| Parameter | Value | Unit |
|---|---|---|
| Gscale | 0.038 | - |
| Gshape | 0.795 | - |
| GscI | 0.018 | - |
| GshI | 1.002 | - |
| PRO | 0.100 | - |
| Cx | 0.0515 | mm/°C/h |
| CFR | 0.00554 | mm/°C/h |
| Cea | 0.0102 | mm/°C/h |
| rv | 1.221 | m/s |
| a0 | 31.92 | - |
| d | 384.1 | - |

## 4.6 Determination of stable stone size

The channel stability in Stabekken is estimated to evaluate its potential for erosion during simulated flood peaks. Maynord's method is used to estimate the stable stone size during a predicted flood. The graphical version of Maynord's method with curves developed by Jenssen and Tesaker (2009) determines the stable stone size in this study. The conditions required to use this method, as described in section 2.6.1, are assumed to be met in Stabekken. The floods predicted in Stabekken using the DDD model in different antecedent catchment conditions with a return period of 200 years are used to determine the stable stone size. It is recommended to use a return period of 200 years to achieve adequate erosion safety (Fergus et al., 2010), hence this is the return period used when estimating the stable stone size in Stabekken. The water depth occurring during the simulated floods are computed via the relationship between observed water depth ($y_0$) and Manning's-transformed discharge ($Q$). The water velocity ($V$) is determined by the relation $V = \frac{Q}{A}$, where $A$ is the area of the stream cross section during a simulated flood. Uniform flow is assumed when using Manning's formula, which leads to uncertainty in parameters in the stable stone size computations. Hence, the graphical version of Maynord's method is found adequate in this study. Figure 2.2 is used to determine $D_{30}$ for the 200-year floods predicted using the DDD model in dry, wet and during snowmelt antecedent soil moisture conditions, and with and without a 40% climate factor.

# 5 Results and discussion

The following objectives were established and set out to be addressed:

- Evaluate the hydrological performance of the infiltration swale established along Rv3.
    - Set up and test a hydrological model that includes the road runoff and the swale.
    - Use the model and the available measurement data to evaluate the performance of the swale.
- Set up and test a hydrological model of the rearranged part of Stabekken using the DDD model and evaluate its applicability for flood estimation in small ungauged catchments.
    - Estimate flow peaks in Stabekken in different antecedent soil moisture conditions.
    - Evaluate the model's applicability in Stabekken using measured water stage data.
    - Estimate and evaluate the channel stability in the rearranged part of Stabekken during a predicted flood peak.

## 5.1 Evaluation of the swale's hydrological performance

The measured water level data are presented, analysed, and used to evaluate the swale's hydrological performance. The results from the SWMM model simulations, besides the limitations of the model and the evaluation, are presented.

### 5.1.1 Water level data within the swale

The HOBO MX2001 Data Loggers that measure the water level within the swale with a time resolution of 10 minutes give useful information on the performance of the swale. The locations of the sensors are illustrated in Figure 4.1. The collected water level data from sensors located at positions P2, P3 and P4, from the period between 30$^{th}$ of July 2020 and 18$^{th}$ of May 2021, are presented in Figure 5.1. Data from the sensors located at P1, P5 and P6 are presented in Appendix C (Figure **0.1**, Figure **0.2** and Figure **0.3**). Water level data between the 1$^{st}$ and 16$^{th}$ of April 2021 are absent due to the sensors being full and not able to read more data in this period. Data from sensor depth 0.75m in sensor position P2 are also missing between 5$^{th}$ of November and 1$^{st}$ of April due to an unknown error. In March 2021, unexpected values are detected in the sensor at depth 0.75m in sensor position P4. Measurement noise is a probable cause of this, however, the exact reason is unknown.

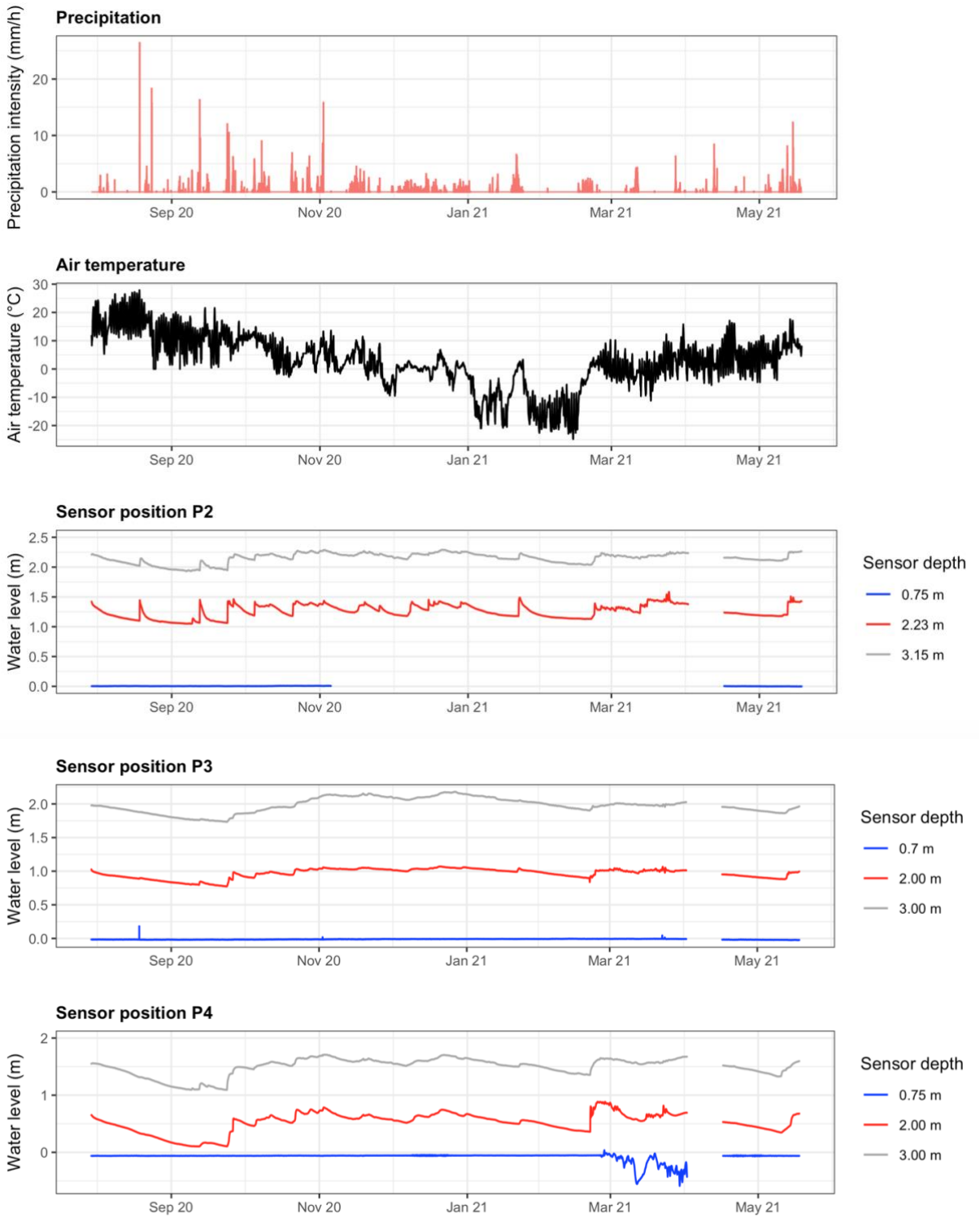


Figure 5.1 Plot showing precipitation, air temperature and measured water levels within the swale at sensor positions P2, P3 and P4 in the period from 30th of July 2020 to 18th of May 2021 (Plotted using R script found in Appendix B).

Infiltration of precipitation and road runoff into the swale, leading to reduction of swale runoff volume and peak runoff delay, are the expected behaviour of the grass swale along Rv3. As seen in Figure 5.1, the water levels within the swale are higher in the sensors located further upstream than the sensors located further downstream in the swale. This indicates that the runoff

volume is reduced due to infiltration of precipitation and runoff in the swale. The lowest sensors, located 0.7m and 0.75m below the swale surface, never measure water levels above zero during the monitoring period. This indicates that all precipitation and road runoff are infiltrated into the swale, that nothing runs off from the swale, and that the soil's infiltration capacity is never exceeded during the monitoring period.

The coherence between precipitation and water levels, and water level patterns in the different plotting positions are discussed to evaluate further the swale performance based on measurement data. The expected behaviour is an increase in water levels within the swale when a rain event of some magnitude occurs. Visual inspection of the precipitation data obtained from Rv3-Stabekken climate station and the water level data show some correlation as the water levels within the swale increase when rain events occur. An example where a rain event co-occurs as water levels increase can be seen in May 2021 and at the end of February 2021, in Figure 5.1. This coincides with the expected behaviour of the swale.

Visual inspection of Figure 5.1 show more rapid movement of the water levels in position P2 than in the further downstream positions, e.g. P3 and P4. The water level response to precipitation events in P2 is faster than in the downstream sensors, indicating that the swale dampens the effect of rain events, hence performing as expected. Differences in water level patterns between the different sensor positions can however also be caused by different soil conditions at the different positions. The lack of data on the soil in the swale makes it challenging to know whether the differences are caused by different soil conditions along the swale or the dampening of precipitation. There are no available data on the infiltration potential of the soil used in the swale. Infiltration measurements were not conducted during fieldwork, which can be seen as a limitation since this type of data is valuable for validation of the sensor measurements and the modelling of swale runoff.

The swale established along Rv3 is located in a cold climate region with low temperatures and snow during winter, which influences its operation and performance. The sensor data indicate that the operation during the winter 2020/2021 was sufficient. The swale managed the snowmelt despite probable accumulation of pollutions and sediment in the snow, which may lead to clogging of the filter material and reduced infiltration capacity (Fach et al., 2011).

Infiltration measurements taken before and after winter season will give information on the hydraulic conductivity and its possible reduction caused by accumulated sediments. This was the case for Fach et al. (2011), where the performance of grass swales during winter times in Alpine regions were studied. Such data are, however, not available for the swale along Rv3. Infiltration capacity data will also be valuable to obtain whether the drainage capacity is sufficient to avoid concrete frost which reduce the swale's performance during winter (Muthanna et al., 2007). The operation of the swale does nevertheless seem sufficient during winter times based on the available data series. The precipitation events are of lower magnitude and intensity during winter, compensating for the potential reduced infiltration capacity due to accumulated pollutions in snow stored on the swale surface (Fach et al., 2011). However, a

longer time series will be valuable to monitor and evaluate the swale's performance during several winter seasons.

### 5.1.2 SWMM model results

A model simulating the swale's hydrological performance during extreme rain events are modelled using SWMM. The model includes the swale and road area that drain into the swale. The simulated swale runoff is presented by the outlet node's total inflow, which drains water from the upstream road and swale subcatchments. A long-term precipitation simulation with precipitation data from the monitoring period between 30th of July 2020 and 18th of May 2021 was run. The infiltration parameters were modified to give a simulation result that coincides with the water level measurements within the swale. The lowest achieved swale runoff is presented in Figure 5.2. As seen from the figure, the runoff from the long-term precipitation simulation is almost zero. However, changing the infiltration parameters did not result in entirely zero runoff which was indicated from the sensor data. The simulated runoff is nevertheless low, and the same model parameters are used when modelling the single storm events.

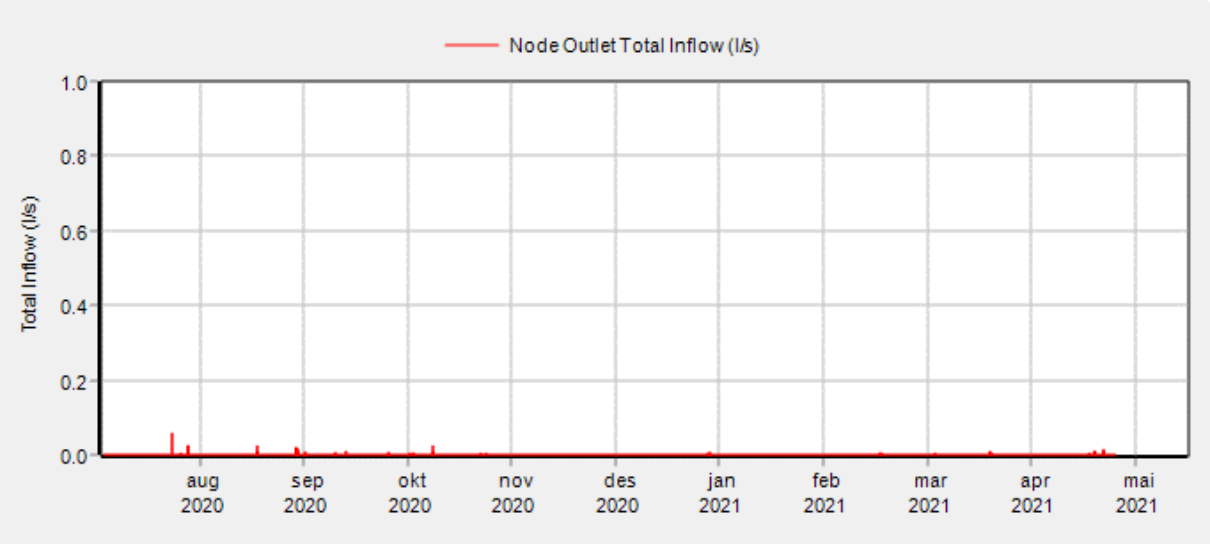


Figure 5.2 Total inflow (l/s) in the outlet node when running a long-term precipitation simulation of the swale model from 30th of July 2020 to 18th of May 2021. Max total inflow = 0.05 l/s. (From SWMM).

For the single storm event simulations, the model is run with 20- and 200-years design rain events with a duration of 60 minutes, including a 40% climate factor. The design events are presented in Figure 4.5. The 20-year return period simulation, including 40% climate factor, resulted in a runoff peak of *1.11 l/s*, as shown in Figure 5.3. Running the 200-year return period simulation, including 40% climate factor, gave a peak inflow into the outlet node equal to *4.37 l/s* as presented in Figure 5.4. The peaks occur approximately 45 minutes after the start of the rain event. The simulation results obtained using 20- and 200-years design events without 40% climate factor are presented in Appendix A (Figure **0.1** and Figure **0.2**). The results indicate relatively little runoff during extreme rainfall events and hence good hydrological performance of the swale. However, there is uncertainty associated with the model due to a lack of data on

soil properties and outflow data. The sources of uncertainty and limitations of evaluating the swale performance are presented and discussed in the following sub-chapter.

Information on where the runoff from the swale drains and possible affected areas downstream are not known. However, the downstream areas are not heavily urbanised and includes mainly pervious areas such as forest areas and agricultural land. Hence, runoff from the swale will not lead to significant negative consequences in the downstream area. If the area was densely urbanised with mainly impervious areas which generate fast runoff, the consequences of an extreme rain event would be more severe.

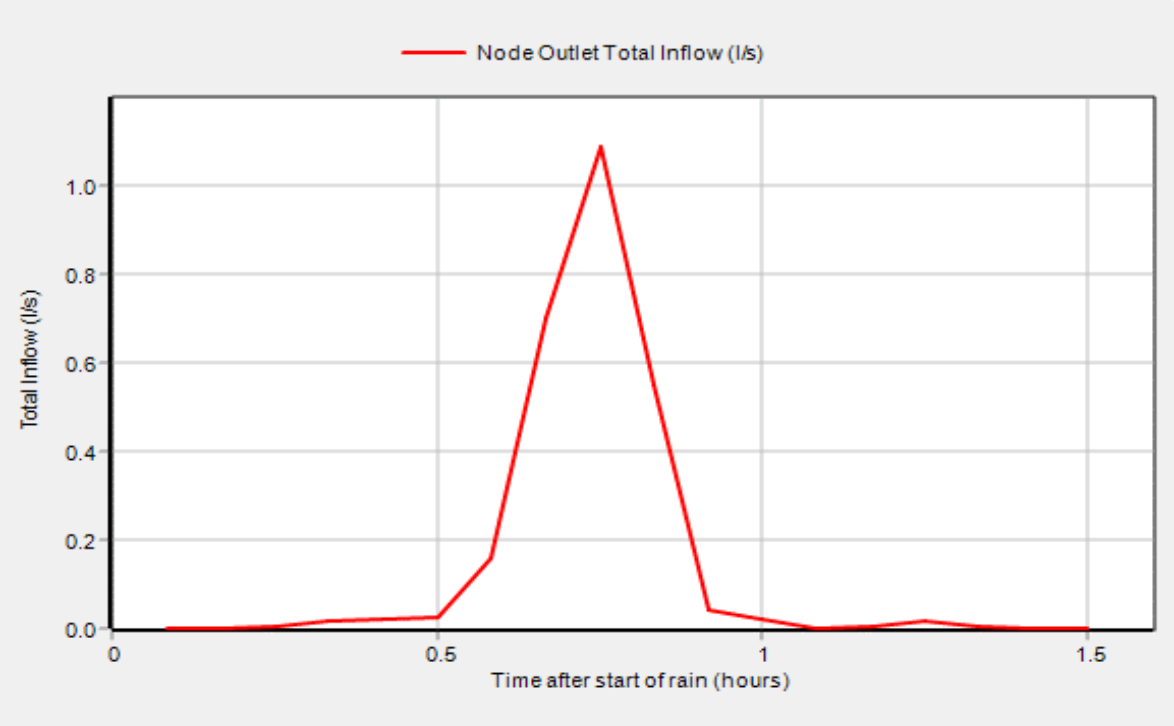


Figure 5.3 Total inflow (l/s) in the outlet node when running a single storm event simulation of the swale model using a 20-years design rain event including 40% climate factor with a duration of 60 minutes. Max total inflow = 1.11 l/s. (From SWMM).

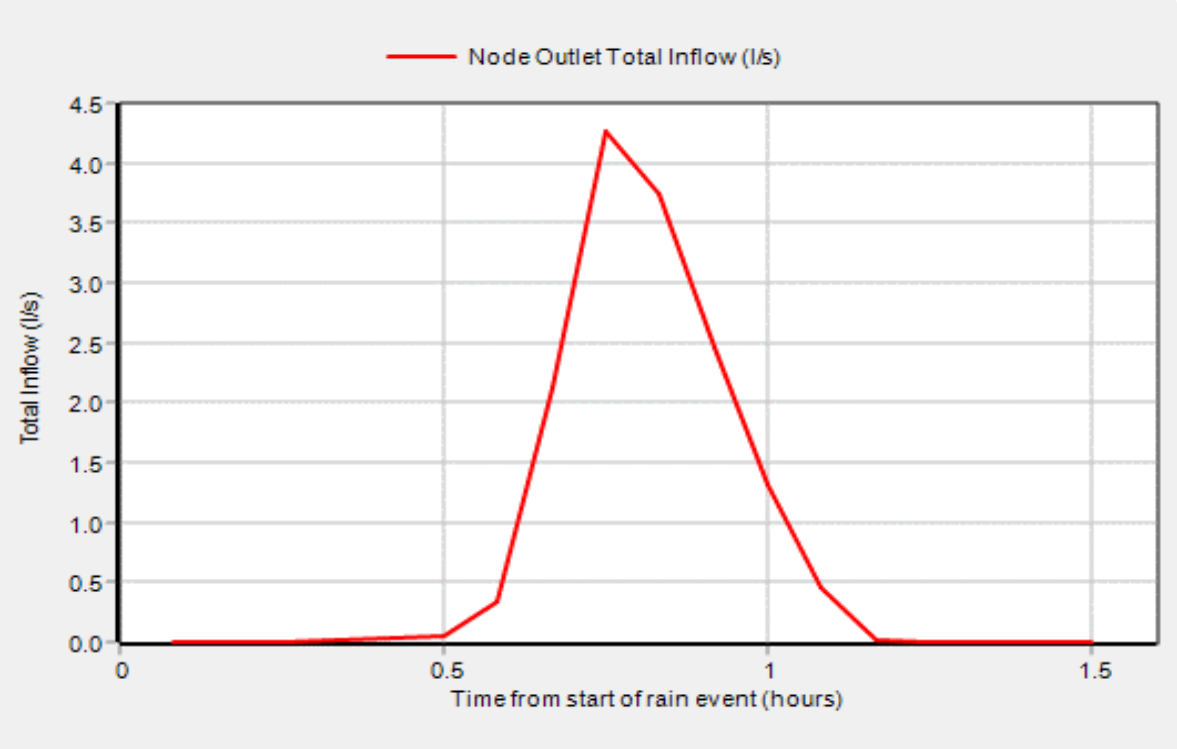


Figure 5.4 Total inflow (l/s) in the outlet node when running a single storm event simulation using a 200-years design rain event including 40% climate factor with a duration of 60 minutes. Max total inflow = 4.37 l/s. (From SWMM).

### 5.1.3 Limitations

Detailed data on the soil properties of the materials used in the built swale along Rv3 are not available. This is a limitation to the study since it leads to large uncertainty in the infiltration parameters, leading to uncertainty in the model results. Hence, infiltration parameters are chosen mainly based on literature. Soil properties data would provide a more reliable assessment of the infiltration parameters of the model. Availability of such data could have hence contributed to decreased uncertainty in the model.

The uncertainty and lack of information regarding the built swale and its materials and structure are important limitations when evaluating the efficiency and capacity of the swale along Rv3. Bergseng (2021) conducted a preliminary study on the treatment efficiency of the swale along Rv3. During the work, information on the project site was obtained, and the study site was found not to be preferable for further research on the swale's treatment efficiency. Some reasons for this was mentioned by Bergseng (2021):

> "The complete overview of how the infiltration swale is built are lacking. Although the swale should have been built according to N200, the presence of rocks in the topsoil indicates that this has not been the case. The thickness of the filter is not known, and under construction it was no particular control of the filter depth.
>
> Another challenge at the Rv3 pilot is that the swales are not controlled during and after construction. It is hard to evaluate performance and reliability when it is not known what is built."

This verifies the challenge associated with the lack of information at the study site. During fieldwork, it was found that instruments measuring the outflow from the swale, which were planned, were not present at the study site. Such outflow data are valuable data for the validation and calibration of the model. No availability of such data limits the possibilities of using the model results to evaluate the swale's performance.

Discrepancies between the planned and built swale may increase the risk of flooding in surrounding areas and pollution of receiving waters if the built swale facilitates less reduction of stormwater quantity and pollution than planned. It is therefore essential to perform controls of the installed infrastructure and detect deviations.

Rv3 is a busy road with AADT > 5000, which leads to polluted runoff. This increases the potential of clogging of the filter material within the swale. The choice of filter material is essential to decrease clogging and enable sufficient infiltration into the swale. Clogging of the swale may occur after some time. With longer time series from the water level sensors, the effects of potential clogging and real extreme events can be observed and evaluated. Longer-term data and appropriate calibration data, such as data on outflow and soil properties, will therefore improve the evaluation of the performance of the infiltration swale.

The water level measurements within the swale and the model results indicate adequate infiltration and dampening of precipitation, and sufficient capacity during winter, thus good hydrological performance. Due to model uncertainty as described previously, it is however difficult to conclude that the swale is 100% effective during extreme rainfall events.

## 5.2 Modelling Stabekken using the DDD model

The DDD model is used to estimate flow in Stabekken. Modelling results, evaluation of its applicability and stable stone size in the rearranged part of the stream are presented and discussed in the following sub-chapters.

Two different parameter sets are tested when running the DDD simulations in Stabekken. Figure 5.5 shows the simulated discharge in Stabekken between 1st of January 2018 and 31st of December 2020. Regression and physical similarity are used in this simulation as regionalisation methods (combined method), as Tsegaw, Alfredsen, et al. (2019) described, to obtain the recession- and calibration parameters, respectively. For the hydrograph presented in Figure 5.6, both recession parameters (*Gscale, Gshape, GscI* and *GshI*) and calibration parameters (*PRO, Cx, CFR, Cea* and *rv*) are transferred directly from the calibrated parameter set used when modelling Fura river (Tsegaw, Alfredsen, et al., 2019). Stabekken is a part of Fura river, hence there are similarities between the gauged and ungauged catchments, and Fura is used as a single donor catchment.

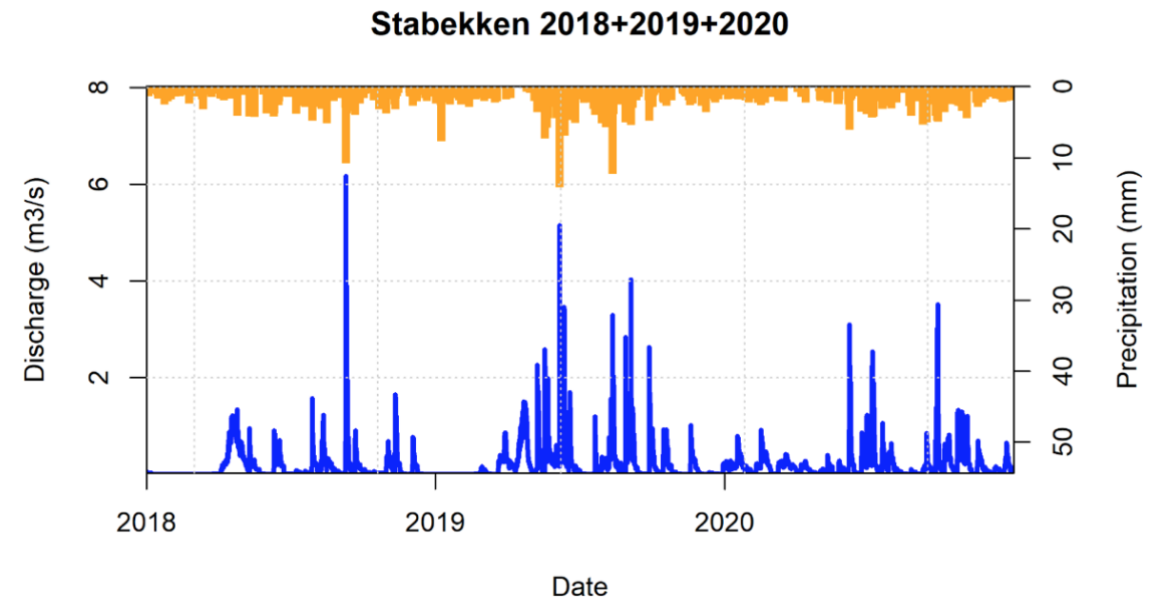


Figure 5.5 Simulated discharge ($m^3/s$) in Stabekken (blue line) in period 1st of January 2018 to 31st of December 2020 with combined method of regionalisation (recession parameters estimated from regression and calibrated parameters from physical similarity method). The orange bars at the top of the plot represent the precipitation input in the model.

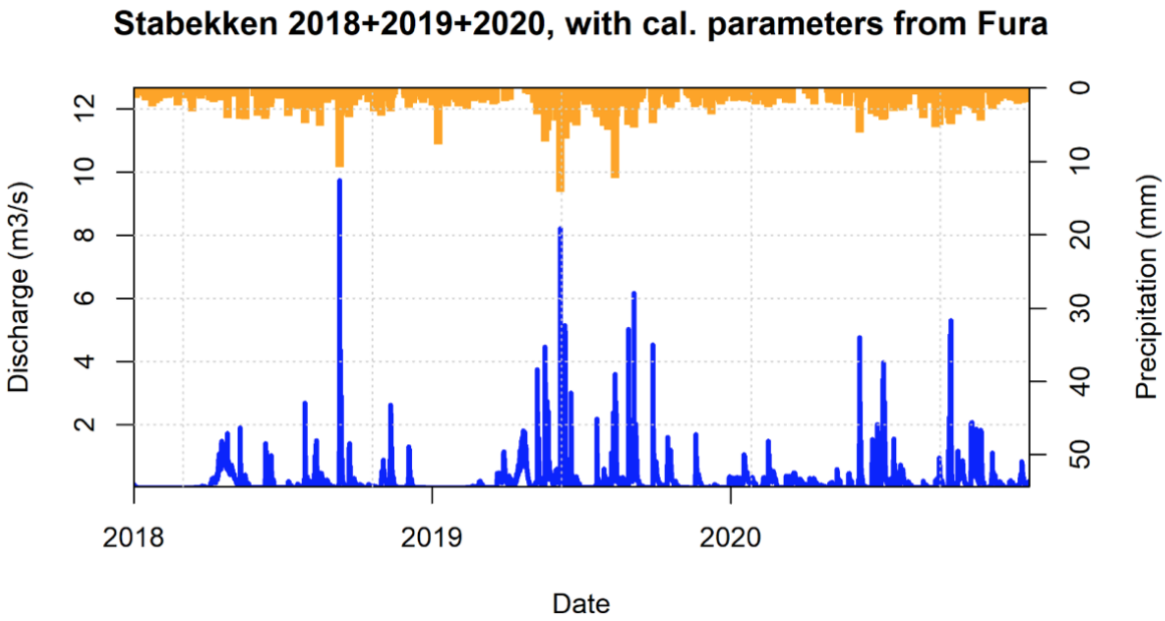


Figure 5.6 Simulated discharge ($m^3/s$) in Stabekken (blue line) in period 1st of January 2018 to 31st of December 2020 with both recession- and calibration parameters transferred directly from Fura. The orange bars at the top of the plot represent the precipitation input in the model.

There are evident differences between the hydrographs simulated using the different parameter sets. The discharge values from the simulation using the combined method are smaller than the discharge values simulated using Fura's parameters. The modelled maximum flood peaks in 2018 are *6.17 m3/s* and *9.73 m3/s* for the combined method and the Fura parameters, respectively. This shows that recession parameters (*Gscale, Gshape, GscI* and *GshI*) are

sensitive parameters and that the choice of regionalisation methods is essential for the model results.

Since the combined method of regionalisation is recommended by Tsegaw, Alfredsen, et al. (2019) for estimating flow in small ungauged catchments in Norway with an hourly temporal resolution, this is used for further DDD model simulations in this study.

### 5.2.1 Flood peaks in different antecedent soil moisture conditions

The DDD model is a continuous model that can include design rain events at different times of the year with different antecedent soil moisture conditions found through simulation. Soil moisture is non-linear related to runoff and plays an important role in runoff generation in a catchment (Penna et al., 2011). The magnitude of a flood depends on the saturation level of the catchment and water level in the stream at the start of the rain event. A higher level of subsurface storage, higher antecedent soil moisture, is associated with higher flood peaks when a rain event occurs since soils in a dry catchment can store amounts of water before surface flow occurs.

Design rain events with 200-year return periods and with and without 40% climate factor are used when modelling flood peaks in Stabekken. These design events are presented in Figure 4.6. The different design events are included in the PTQ-file during different soil moisture conditions (dry, wet and during snowmelt) when running the DDD model simulations.

The dry catchment condition is identified by running the DDD model from 2018 to 2020 without design rainfall events and finding a period with a combination of little precipitation, high temperatures and low flow in Stabekken. This was found on 8$^{th}$ of July 2018. The results of the simulations with flood peaks in dry antecedent soil moisture conditions are presented in Figure **5.8**. The results of the simulations with flood peaks in wet catchment conditions, 10$^{th}$ of September 2018, identified by finding a period with precipitation and high flow in Stabekken, are presented in Figure **5.9**. A snowmelt period was identified by investigating the snow storage in the catchment, shown in Figure 5.7, and choosing a period where the snow storage decreases, e.g. on 18$^{th}$ of April 2019. The results from the flood peak simulations during snowmelt is shown in Figure **5.10**. The flood peak discharge values are presented in Table 5.1.

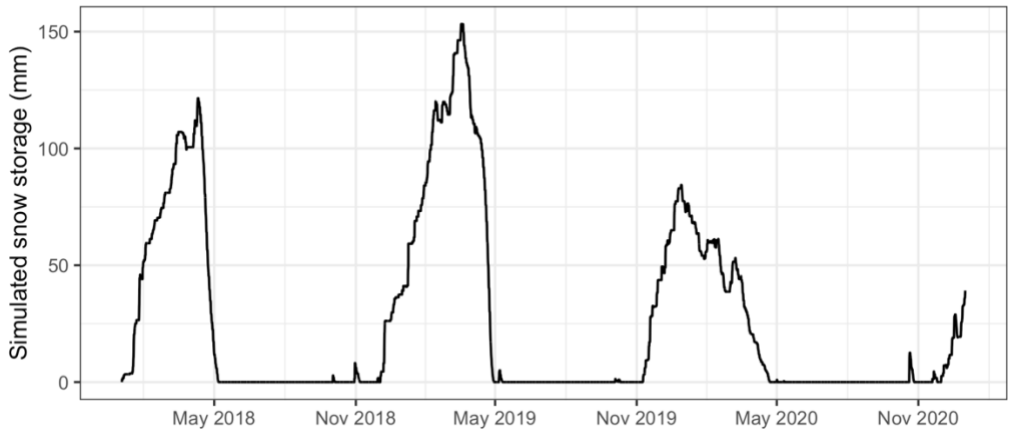


Figure 5.7 Simulated snow storage (mm) (from the DDD model) in Stabekken in the period from 1st of January 2018 to 31st of December 2020.

Table 5.1 Flood peaks simulated for 2018-2020 with different antecedent soil moisture conditions. 200-year design rain events both with and without 40% climate factor are used.

| Antecedent soil conditions | Design rain event | Flood peak ($m^3/s$) |
|---|---|---|
| Dry | 200-year design rain | 16.64 |
| | 200-year design rain incl. 40% climate factor | 29.61 |
| Wet | 200-year design rain | 22.13 |
| | 200-year design rain incl. 40% climate factor | 35.29 |
| Snowmelt | 200-year design rain | 22.34 |
| | 200-year design rain incl. 40% climate factor | 35.17 |

The results show that the flood peaks predicted with dry antecedent soil moisture conditions are smaller than with wet antecedent catchment conditions and during snowmelt. This is consistent with results found in literature (James & Roulet, 2009; Penna et al., 2011) that the antecedent soil moisture is an essential factor for the runoff generation. In Stabekken, the flood peaks modelled in wet antecedent catchment conditions are up to 33% higher than the flood estimated in dry conditions when using the same design precipitation event.

When using a continuous model such as the DDD model, antecedent soil moisture conditions are found through model simulation. Hence, actual conditions, such as the present snow storage, can be accounted for when predicting floods. This is not the case for typically used event-based methods, such as the rational formula and PQRUT, where the antecedent moisture conditions are set manually. Lawrence et al. (2014) found that continuous models estimate data that is closer to data based on flood frequency analysis than other common simulation methods. Continuous models are therefore preferred to increase the prediction accuracy.

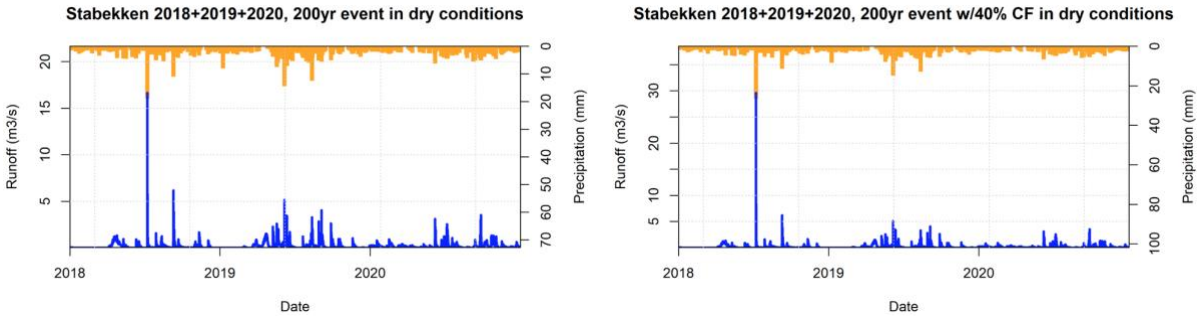


Figure 5.8 Simulated discharge ($m^3/s$) in Stabekken in period 1st of January 2018 to 31st of December 2020 including a 200-year design rain event without (left figure) and with (right figure) 40% climate factor when there are dry soil conditions on 8th of July 2018.

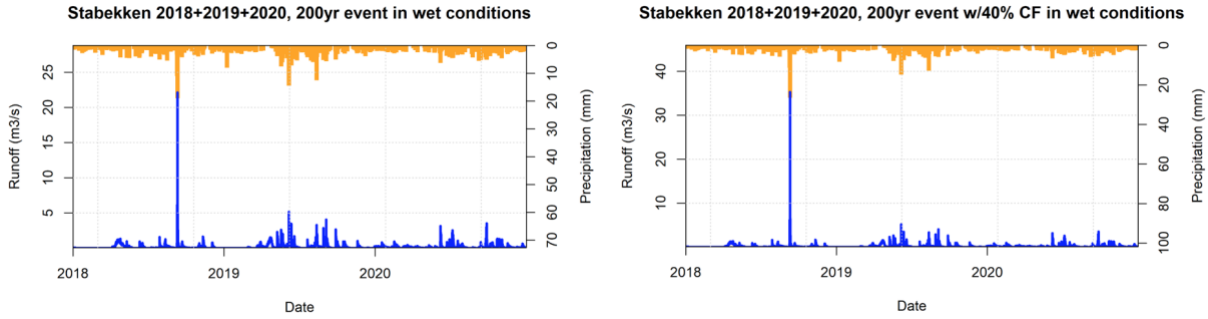


Figure 5.9 Simulated discharge ($m^3/s$) in Stabekken in period 1st of January 2018 to 31st of December 2020 including a 200-year design rain event without (left figure) and with (right figure) 40% climate factor when there are dry soil conditions on 8th of July 2018.

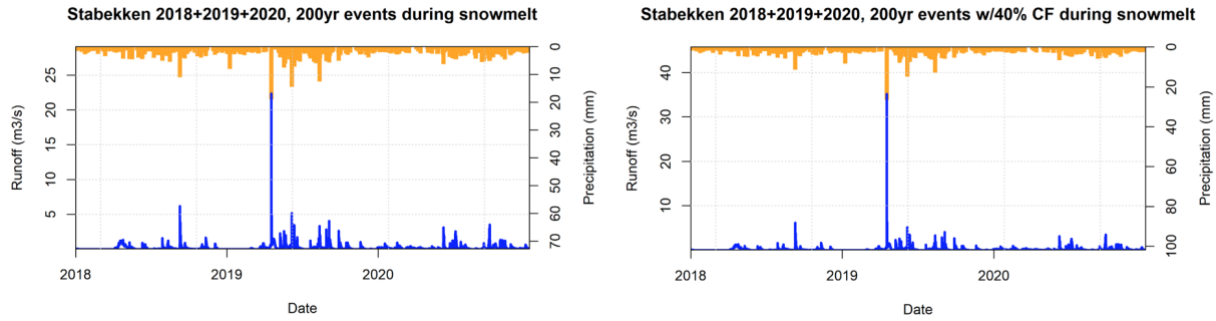


Figure 5.10 Simulated discharge ($m^3/s$) in Stabekken in period 1st of January 2018 to 31st of December 2020 including a 200-year design rain event without (left figure) and with (right figure) 40% climate factor when there are dry soil conditions on 8th of July 2018.

### 5.2.2 Evaluation of prediction accuracy using water stage measurements

An inherent problem in estimating flow in ungauged catchments is the lack of data for assessing the accuracy of the predicted flow. For Stabekken, stage data is measured using TD-Divers, but unfortunately, no stage-discharge curve is established at the measurement point. Thus, no discharge data are available, which would be appropriate for calibration and validation of the model. However, the water stage measurements can be used to evaluate the accuracy of the model by analysing whether it is coherence between the observed water stage and the simulated discharge in regards to patterns and timing of peaks.

The collected water stage data from Stabekken measured with two TD-Divers located upstream and downstream the culvert (see Figure 4.1 for location), between 9th of November 2020 and 18th of May 2021, are presented in Figure 5.11 (Observed water stage). Data between 1st and 22nd of January 2020 are missing due to errors caused by low temperatures. Figure 5.11 also includes climate data collected from Rv3-Stabekken climate station, discharge values converted from the observed water stage using Manning's formula ("observed "discharge) and simulated discharge using the DDD model.

Visual inspection of the figure shows some correlation between detected rainfall and increase in water stage and simulated discharge. Examples of this can be found in the middle of November 2020 and May 2021, where rainfall occur approximately simultaneously as there are peaks in the water stage and simulated discharge. This coincides well with the expected behaviour of the rainfall response in the catchment. When a precipitation event occurs in the middle of January 2021, there is no increase in the water stage or simulated discharge, as seen in Figure 5.11. This can be due to low temperatures, which lead to ice on Stabekken and precipitation as snow. These observations indicate a correlation between the detected rainfall and measured stage, which verifies the quality of this data.

Visual inspection of the water stage data and the simulated discharge data is done to detect a potential coherence and evaluate the model's accuracy. Similarities in the pattern of the plots are found. When there are flood peaks in the simulated hydrograph, similar peaks can be found in the water stage data occurring at similar times. Examples of this can be seen in Figure 5.11 in the middle of November 2020, end of December 2020, end of February 2021, end of March 2021 and middle of May 2021. Coherence between the two time series is therefore detected. The water stage time series has, however, more frequent and distinct peaks than the simulated hydrograph.

Some similarities in the relative magnitude of peaks between the stage and simulated flow are also found through visual inspection of the time series. Examples can be observed in the peaks in March and April 2020. The peaks in March are smaller than in April in the water stage data and the simulated flow. This indicates some validation of the relative magnitude in the simulated discharge.

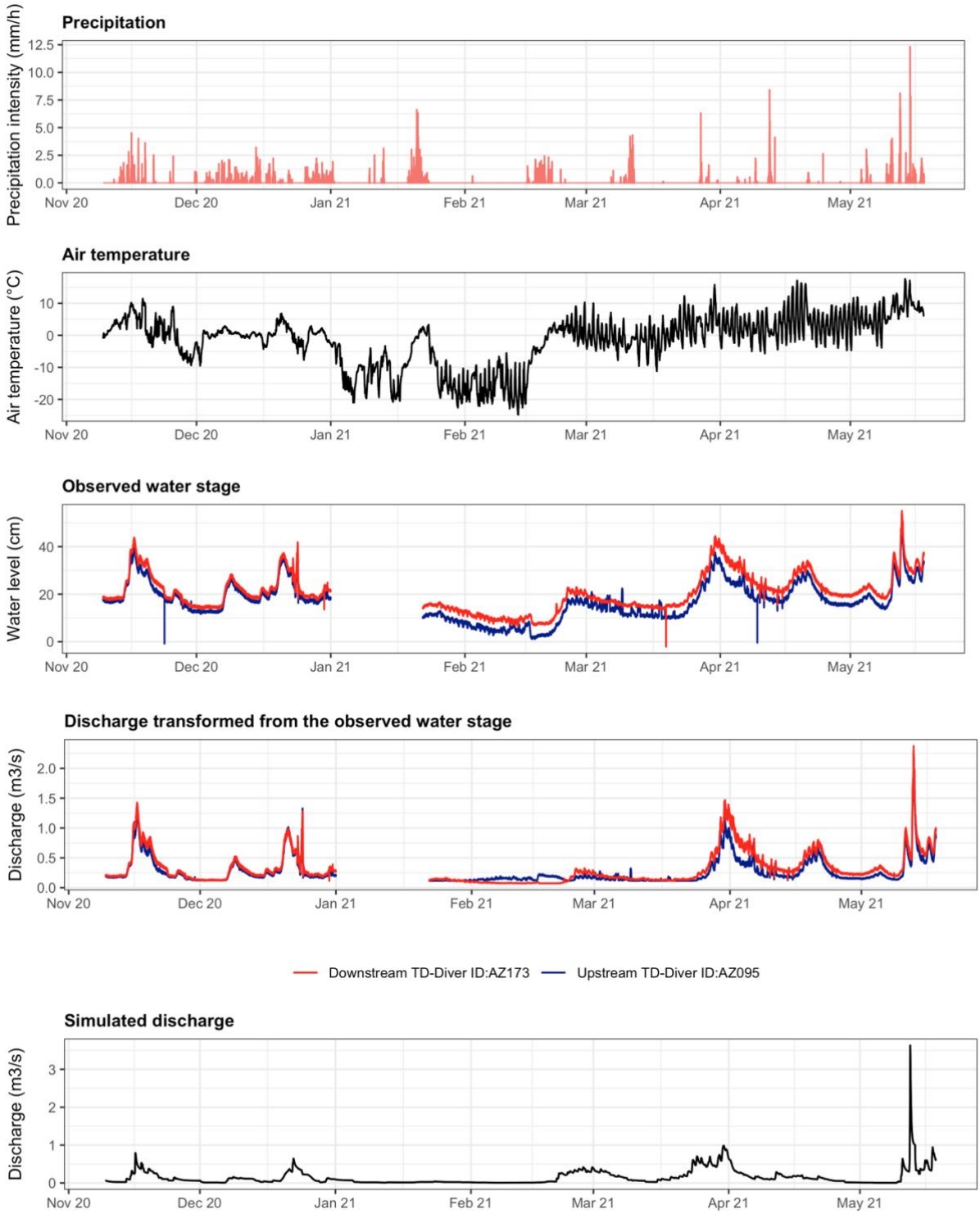


Figure 5.11 Plots of precipitation, air temperature, observed water level in Stabekken measured using TD-Divers, discharge transformed from observed water level in Stabekken and simulated discharge using the DDD model in the period 9th of November 2020 – 18th of May 2021. (Plotted using R script found in Appendix E).

The similarities in trends between the simulated discharge, water stage and precipitation regarding relative magnitude and timing of peaks indicate coherence and verification of the trends in the model results. However, the exact magnitudes of the simulated floods cannot be

evaluated due to uncertainties in the "observed" discharge values that make it not appropriate for direct comparison. Manning's formula was used to convert the observed water stage in Stabekken to estimated "observed" discharge, as described in sub-chapter 4.1.1. Many assumptions were made in the conversion from stage to discharge, such as uniform flow. The choice of Manning's n-value was also based on assumptions due to little available data. Due to the uncertainty in these assumptions, it is decided not to use the "observed" discharge for further evaluation and validation of the model accuracy. For the period presented in Figure 5.11, the model simulates mainly lower discharge values than the "observed" discharge. However, exceptions occur in March and May 2021, where the simulated discharge values are higher than the "observed" values from the downstream measurement point. Due to uncertainties in both the "observed" and simulated discharge, no conclusions are made on which is most accurate. The DDD model is nevertheless found suitable for the modelling purpose, at least partly due to validation of relative magnitude and timing of peaks, using the measure water stage.

The prediction accuracy in flood estimation methods for ungauged catchments is often better for hydrological models such as the DDD models with regionalisation methods than for model-independent methods, such as scaling. Elhadi (2019) studied the accuracy of several flood estimation methods in small ungauged catchments, such as scaling and different regionalisation methods using the HBV and DDD model. Results from that study showed that scaling generated the least accurate prediction results. Scaling are associated with more significant uncertainty than methods that take more catchment features and processes into consideration, such as the HBV and DDD model that use regionalisation methods. The DDD model with the combined regionalisation method (regression and physical similarity) was found to predict satisfactory model results in small catchments in previous studies (Elhadi, 2019; Tsegaw, Alfredsen, et al., 2019). Hence, it is reasonable to assume that the DDD model with the combined regionalisation method is suitable for flood prediction in Stabekken. The promising results on timing and relative magnitude of peaks from the model evaluation using water stage data in Stabekken substantiate this statement.

### 5.2.3 Evaluation of channel stability in Stabekken

Due to the establishment of Rv3, Stabekken was rearranged to avoid crossing the road. The stable stone size in this part of the stream is hence estimated and evaluated to study the effect of the predicted floods in the rearranged part of Stabekken.

The stable stone size in Stabekken is estimated using the graphical version of Maynord's method as described in sub-chapter 4.6. The upstream cross section measured with GNSS instruments during fieldwork, as described in sub-chapter 4.1, is used as the cross section where stable stone size is computed. Table 5.2 shows the estimated stone size $D_{30}$ for different flow scenarios. The particular flow scenarios are simulated floods using the DDD model with 200-year design rain events with and without 40% climate factor in both dry and wet antecedent soil moisture conditions (see Table 5.1 for flood peaks).

Table 5.2 The stone size $D_{30}$ estimated using the graphical Maynard's method. Different flood scenarios are considered to estimate the stone size $D_{30}$ with and without climate factor in bot dry and wet antecedent soil moisture conditions.

| **Antecedent soil moisture** | Dry | | Wet | |
|---|---|---|---|---|
| **Flood scenario** | Q200 | Q200+40%CF | Q200 | Q200+40%CF |
| $D_{30}$ **(m)** | 0.08 | 0.125 | 0.09 | 0.15 |

Large uncertainty is connected to the estimation of the stable stone size in Stabekken. The most important parameters in stone size computations are water velocity, stone density, side slope, and water depth. The water velocity is the most sensitive parameter. With a 10% increase in velocity, the weight of stones and thickness must be increased by 100% and 30%, respectively, to resist the same floods and avoid erosion (Jenssen & Tesaker, 2009). The water velocity in this study is calculated using Manning's formula, which also is connected to uncertainty.

Pictures taken during fieldwork showing the stones in the side slopes and on the bottom of the rearranged part of Stabekken are presented in Figure 5.12. The exact stone size values and size distribution in the rearranged part of Stabekken are not known. This is a limitation to the channel stability evaluation on whether the stones present in Stabekken are sufficient to avoid erosion during a flood with a return period of 200 years. Through observation, it can, however, look like the stones present in Stabekken are in the same size range as the estimated values $D_{30}$. If so, the channel stability of the rearranged part of Stabekken is sufficient to avoid erosion and changed flow pattern during a 200-year flood. Only particle erosion is evaluated in this study. Particle erosion is only a contributing factor to the overall erosion process (Brown & Clyde, 1989). More erosion processes should be investigated, more detailed data on the stones at site and computations parameters should be available to conduct a complete channel stability evaluation.

Figure 5.12 Pictures of the rearranged part of Stabekken. The stones in the side slopes (left pictures) and on the bottom (right pictures) of the stream can be seen in the pictures (Photos by: Kristine Bergseng).

The objective of evaluating channel stability and stable stone size in Stabekken is to check if the existing stones in Stabekken are sufficient to avoid erosion during floods simulated with the

DDD model. Due to uncertainty connected to the estimated stone sizes and the size of the stones on site, no distinct conclusion can be made on the channel stability of Stabekken.

# 6 Conclusions

This study set out to model and evaluate the hydrological performance of an infiltration grass swale and a rearranged stream along Rv3 between Ommangsvollen and Grundset. The swale was established to reduce the quantity and improve the quality of road runoff, and provide stormwater transport. The swale evaluation conducted in this study focuses on the hydrological effectiveness of the swale. Hydrological modelling of the stream is done using the Distance Distribution Dynamics (DDD) model to assess its applicability for flow prediction in small ungauged catchments.

Water level data within the swale from 31st of July 2020 to 18th of May 2021 are available and analysed to evaluate the hydrological performance of the swale. These measurements indicate that all road runoff is infiltrated in the swale during this period, as well as dampening of precipitation events and adequate hydrological performance during the observed winter season. This suggests good performance of the swale regarding the quantity, volume reduction, of runoff.

A model simulating the swale runoff is made using Storm Water Management Model (SWMM). The swale drains the road and receives road runoff. Based on the water level measurements that indicate no runoff from the swale, the model is set up with infiltration parameter values such that the model simulates nearly zero runoff during the monitoring period. When running the single storm events with design rain events with return periods of 20 and 200 years, the model indicate little swale runoff, hence good performance. However, the model is not calibrated and has large uncertainty due to a lack of outflow and soil properties data. It is not easy to make distinct conclusions regarding the swale's hydrological efficiency during extreme rainfall events. A similar stormwater management system can be recommended in similar road projects based on the promising results regarding the swale's hydrological performance. However, this only applies to the hydrological efficiency and infiltration of the swale since its treatment efficiency has not been assessed.

The DDD model is used to estimate flow and predict floods in the rearranged part of Stabekken. Flood prediction in small ungauged catchments is associated with large uncertainty and serves as a challenge in hydrology since flow data is lacking. A combined regionalisation method (regression and physical similarity) is used in Stabekken when modelling design floods in different antecedent soil moisture conditions. The greatest flood peak is modelled in wet catchment conditions. The 200-year flood peak, including 40% climate factor, modelled in wet catchment conditions, are 33% greater than the flood peak modelled in dry conditions using the same design rainfall event. Such flood peak modelling where the antecedent soil moisture conditions are determined through simulation is possible in continuous models but not in typical event-based models. This is a valuable feature in continuous models such as DDD.

The DDD model's applicability in Stabekken is evaluated based on available water stage data from Stabekken and the simulated discharge during the monitoring period (9th of November 2020 to 18th of May). Similarities in timing and relative magnitude of peaks between the stage

data and simulated flow indicate that DDD with the chosen regionalisation methods (combined method) are suitable for flood prediction in Stabekken. However, the magnitude of the simulated floods cannot be assessed directly due to no observed flow data. Based on the evaluated applicability of the DDD model in Stabekken, and previous applications of the model in regionalisation studies, it is favourable for flood estimation in small ungauged catchments.

Uncertainty is associated with the estimated stable stone size and the present stone sizes in and along Stabekken. However, the estimations show that the channel stability in Stabekken is sufficient to avoid erosion during a 200-year flood.

## 6.1 Recommendations for future work

To improve the evaluation of the hydrological performance of the swale and decrease the model uncertainty, infiltration measurements of the swale are suggested. This will give more information on the soil and its infiltration capacity. Potential reduction in hydraulic conductivity, which may happen during winter season, can be obtained by doing infiltration measurements both before and after winter. This and longer time series of water level data will give further information on the swale's long-term performance, including the effects of cold climate and maintenance needs. This will contribute to research on grass swales in cold climates, which is helpful due to few specific design criteria.

Outflow data from the swale will enable calibration and validation of the swale model, hence more accurate modelling and assessment of the swale's hydrological performance during design rain events.

To improve the assessment of the accuracy of the predicted flow in Stabekken, a stage-discharge curve can be developed. This can be done by measuring some discharge values at the same location as the TD-divers, which measure stage. This will be useful for further evaluation of the DDD model's applicability in small ungauged catchments such as Stabekken. Simplifying the user interface and set up of the DDD model is recommended to make it easier to use and more accessible for dimensioning and practical analysis.

# References


Balston, J., Li, S., Iankov, I., Kellett, J., & Wells, G. (2017). Quantifying the Financial Impact of Climate Change on Australian Local Government Roads. *Infrastructures, 2*(1), 2. https://doi.org/10.3390/infrastructures2010002

Bergseng, K. (2021). *Roadwater Treatment in Swales and Vulnerability of Recipient - a site study at Rv3, Stabekken* [Specialisation project]. Norwegian University of Science and Technology [Unpublished].

Blöschl, G., & Sivapalan, M. (1995, 04/01). Scale issues in hydrological modelling: A review. *Hydrological Processes, 9*, 251-290. https://doi.org/10.1002/hyp.3360090305

Brown, S. A., & Clyde, E. S. (1989). *Design of Riprap Revetment*. https://www.usbr.gov/tsc/techreferences/hydraulics_lab/pubs/PAP/PAP-0798.pdf

Caraco, D., & Claytor, R. (1997). Stormwater BMP Design Supplement for Cold Climates. *Center for Watershed Protection, Ellicott City, MD*, 1-96. https://www.in.gov/indot/files/BMP_Design_Cold_Climates.pdf

Chow, V. T. (1959). *Open channel hydraulics*. MCGraw Hill Book company Inc.

Chow, V. T., Maidment, D. R., & Mays, L. W. (1998). *Applied Hydrology*. McGraw-Hill Book Company Inc.

Damodaram, C., Giacomoni, M. H., Prakash Khedun, C., Holmes, H., Ryan, A., Saour, W., & Zechman, E. M. (2010). Simulation of Combined Best Management Practices and Low Impact Development for Sustainable Stormwater Management1. *JAWRA Journal of the American Water Resources Association, 46*(5), 907-918. https://doi.org/10.1111/j.1752-1688.2010.00462.x

Davis, A. P., Stagge, J. H., Jamil, E., & Kim, H. (2012). Hydraulic performance of grass swales for managing highway runoff. *Water Research, 46*(20), 6775-6786. https://doi.org/10.1016/j.watres.2011.10.017

Devia, G. K., Ganasri, B. P., & Dwarakish, G. S. (2015). A Review on Hydrological Models. *Aquatic Procedia, 4*, 1001-1007. https://doi.org/10.1016/j.aqpro.2015.02.126

Dyrrdal, A. V., & Førland, E. J. (2019). *Climate factor for short-term precipitation (Norwegian title: Klimapåslag for korttidsnedbør)* (5). NCCS.

https://cms.met.no/site/2/klimaservicesenteret/rapporter-og-publikasjoner/_attachment/14869?_ts=16b02bdea3a

Elhadi, M. H. A. (2019). *Evaluating approaches to estimate runoff from small ungauged catchments in Norway* [Master thesis],

Engeland, K., Skaugen, T. E., Haugen, J. E., Beldring, S., & Førland, E. (2004). *Compraison of evaporation estimates by the HIRHAM and GWB models for present climate and climate change scenarios* (17). MET.

Fach, S., Engelhard, C., Wittke, N., & Rauch, W. (2011). Performance of infiltration swales with regard to operation in winter times in an Alpine region. *Water Science and Technology, 63*(11), 2658-2665. https://doi.org/10.2166/wst.2011.153

Fergus, T., Hoseth, K. A., & Sæterbø, E. (2010). *Waterway manual (Norwegian title: Vassdragshåndboka)*. NVE.

Fleig, A., & Wilson, D. (2013). *Flood estimation in small catchments* (Report No. 60-2013). NVE. https://publikasjoner.nve.no/rapport/2013/rapport2013_60.pdf

García-Serrana, M., Gulliver, J. S., & Nieber, J. L. (2017). Infiltration capacity of roadside filter strips with non-uniform overland flow. *Journal of Hydrology, 545*, 451-462. https://doi.org/10.1016/j.jhydrol.2016.12.031

James, A. L., & Roulet, N. T. (2009). Antecedent moisture conditions and catchment morphology as controls on spatial patterns of runoff generation in small forest catchments. *Journal of Hydrology, 377*(3-4), 351-366. https://doi.org/10.1016/j.jhydrol.2009.08.039

Jenssen, L., & Tesaker, E. (2009). *Guideline for dimensioning of erosion control of stone (Norwegian title: Veileder for dimensjonering av erosjonsikring av stein)*. NVE. https://publikasjoner.nve.no/veileder/2009/veileder2009_04.pdf

Kaykhosravi, S., Khan, U., & Jadidi, A. (2018). A Comprehensive Review of Low Impact Development Models for Research, Conceptual, Preliminary and Detailed Design Applications. *Water, 10*(11), 1541. https://doi.org/10.3390/w10111541

Klima2050. (n.d.-a). *About Klima2050*. Retrieved 17. November 2020 from http://www.klima2050.no/

Klima2050. (n.d.-b). *Rv3 - Stormwater management and maintenance needs*. Retrieved 13. April 2021 from http://www.klima2050.no/rv3-stormwater-and-maintenance

Lawrence, D., Paquet, E., Gailhard, J., & Fleig, A. K. (2014). Stochastic semi-continuous simulation for extreme flood estimation in catchments with combined rainfall–snowmelt flood regimes. *Nat. Hazards Earth Syst. Sci., 14*(5), 1283-1298. https://doi.org/10.5194/nhess-14-1283-2014

Lillegraven, M. G. (2020). *Data Collection and Model Selection in Preparation of Modelling Rv3 Swales and Local Catchment* [Specialisation project]. Norwegian University of Science and Technology [Unpublished].

Lussana, C., Saloranta, T., Skaugen, T., Magnusson, J., Tveito, O. E., & Andersen, J. (2018). seNorge2 daily precipitation, an observational gridded dataset over Norway from 1957 to the present day. *Earth System Science Data, 10*(1), 235-249. https://doi.org/10.5194/essd-10-235-2018

MET. (n.d.). *Norwegian observational gridded climate datasets, seNorge2* https://thredds.met.no/thredds/catalog/senorge/seNorge2/provisional_archive/catalog.html

Mishra, P. K., Neelkanth, J. K., Maheswara Babu, B., & Kumathe, S. S. (2006). Effectiveness of Bermuda grass as vegetative cover in grassed waterway: A simulated study. *Journal of Irrigation and Drainage Engineering, 132*(3), 288-292. https://doi.org/10.1061/(ASCE)0733-9437(2006)132:3(288)

Monrabal-Martinez, C., Aberle, J., Muthanna, T. M., & Orts-Zamorano, M. (2018). Hydrological benefits of filtering swales for metal removal. *Water Research, 145*, 509-517. https://doi.org/10.1016/j.watres.2018.08.051

Muthanna, T. M., Viklander, M., Blecken, G., & Thorolfsson, S. T. (2007). Snowmelt pollutant removal in bioretention areas. *Water Research, 41*(18), 4061-4072. https://doi.org/10.1016/j.watres.2007.05.040

Narsimlu, B., Rao, B. V., Mishra, P. K., & Rao, K. V. (2004). Effect of Covers for Soil and Water Conservation Using Tilting Flume. *Journal of Irrigation and Drainage Engineering, 130*(2), 154-159. https://doi.org/10.1061/(ASCE)0733-9437(2004)130:2(154)

NPRA. (2018a). *Road construction (Nowegian title: Vegbygging)* (N200). NorwegianPublicRoadAdministration. https://www.vegvesen.no/_attachment/188382/binary/980128?fast_title=H%C3%A5ndbok+N200+Vegbygging+(21+MB).pdf

NPRA. (2018b). *Rv3 and Rv25 Ommangsvollen–Grundset/Basthjørnet*. The Norwegian Public Roads Administration. Retrieved 13. april 2021 from https://www.vegvesen.no/en/professional/roads/Public+Private+Partnership+PPP/ppp-projects-operated-through-ppp-contracts/ommangsvollengrundset

NPRA. (2020). *Water management, Flood computations and hydraulic dimensioning (Norwegian title: Vannhåndtering, Flomberegninger og hydraulisk dimensjonering)* (V240). NorwegianPublicRoadAdministration. https://www.vegvesen.no/_attachment/2988797/binary/1371938?fast_title=H%C3%A5ndbok+V240+Vannh%C3%A5ndtering+-+Flomberegninger+og+hydraulisk+dimensjonering.pdf

NPRA. (n.d.). *Annual average daily traffic* Retrieved 1. February 2021 from https://www.vegvesen.no/trafikkdata/start/utforsk?datatype=averageDailyYearVolume&daytype=ALL&display=chart&from=2021-06-10&trpids=14709V3106834

O'Loughlin, G., Huber, W., & Chocat, B. (1996). Rainfall-runoff processes and modelling. *Journal of Hydraulic Research, 34*(6), 733-751. https://doi.org/10.1080/00221689609498447

Oudin, L., Andréassian, V., Perrin, C., Michel, C., & Le Moine, N. (2008). Spatial proximity, physical similarity, regression and ungaged catchments: A comparison of regionalization approaches based on 913 French catchments. *Water Resources Research, 44*(3). https://doi.org/10.1029/2007WR006240

Parajka, J., Viglione, A., Rogger, M., Salinas, J. L., Sivapalan, M., & Blöschl, G. (2013). Comparative assessment of predictions in ungauged basins – Part 1: Runoff-hydrograph studies. *Hydrol. Earth Syst. Sci., 17*(5), 1783-1795. https://doi.org/10.5194/hess-17-1783-2013

Penna, D., Tromp-Van Meerveld, H. J., Gobbi, A., Borga, M., & Dalla Fontana, G. (2011). The influence of soil moisture on threshold runoff generation processes in an alpine headwater catchment. *Hydrology and Earth System Sciences, 15*(3), 689-702. https://doi.org/10.5194/hess-15-689-2011

Razavi, T., & Coulibaly, P. (2013). Streamflow Prediction in Ungauged Basins: Review of Regionalization Methods. *Journal of Hydrologic Engineering, 18*(8), 958-975. https://doi.org/10.1061/(ASCE)HE.1943-5584.0000690

Rossman, L. A. (2015). Storm Water Management Model User's Manual Version 5.1. *US EPA Office of Research and Developement*.

Rossman, L. A. (2016). Storm Water Management Model Reference Manual, Volume I - Hydrology (Revised). *US EPA Office of Research and Developement*.

Rushton, B. T. (2001). Low-Impact Parking Lot Design Reduces Runoff and Pollutant Loads. *Journal of Water Resources Planning and Management, 127*(3), 172-179. https://doi.org/10.1061/(ASCE)0733-9496(2001)127:3(172)

Sivapalan, M., Takeuchi, K., Franks, S. W., Gupta, V. K., Karambiri, H., Lakshmi, V., Liang, X., McDonnell, J. J., Mendiondo, E. M., O'Connell, P. E., Oki, T., Pomeroy, J. W., Schertzer, D., Uhlenbrook, S., & Zehe, E. (2003, 2003/12/01). IAHS Decade on Predictions in Ungauged Basins (PUB), 2003–2012: Shaping an exciting future for the hydrological sciences. *Hydrological Sciences Journal, 48*(6), 857-880. https://doi.org/10.1623/hysj.48.6.857.51421

Skaugen, T., & Mengistu, Z. (2016). Estimating catchment-scale groundwater dynamics from recession analysis – enhanced constraining of hydrological models. *Hydrology and Earth System Sciences, 20*(12), 4963-4981. https://doi.org/10.5194/hess-20-4963-2016

Skaugen, T., & Onof, C. (2014). A rainfall-runoff model parameterized from GIS and runoff data. *Hydrological Processes, 28*(15), 4529-4542. https://doi.org/10.1002/hyp.9968

Skaugen, T., Peerebom, I. O., & Nilsson, A. (2015). Use of a parsimonious rainfall–run-off model for predicting hydrological response in ungauged basins. *Hydrological Processes, 29*(8), 1999-2013. https://doi.org/10.1002/hyp.10315

Skaugen, T., & Weltzien, I. H. (2016). A model for the spatial distribution of snow water equivalent parameterized from the spatial variability of precipitation. *The Cryosphere, 10*(5), 1947-1963. https://doi.org/10.5194/tc-10-1947-2016

Stenius, S., Glad, P. A., Wang, T. K., & Væringstad, T. (2015). *Guide for flood estimation in small ungauged basins (Norwegian title: Veileder for flomberegninger i små uregulerte felt)*. NVE. https://publikasjoner.nve.no/veileder/2015/veileder2015_07.pdf

Tsegaw, A. T., Alfredsen, K., Skaugen, T., & Muthanna, T. M. (2019). Predicting hourly flows at ungauged small rural catchments using a parsimonious hydrological model. *Journal of Hydrology, 573*, 855-871. https://doi.org/10.1016/j.jhydrol.2019.03.090

Tsegaw, A. T., Skaugen, T., Alfredsen, K., & Muthanna, T. M. (2019). A dynamic river network method for the prediction of floods using a parsimonious rainfall-runoff model. *Hydrology Research, 51*(2), 146-168. https://doi.org/10.2166/nh.2019.003

Wilson, D., Fleig, A. K., Lawrence, D., Hisdal, H., Pettersson, L.-E., & Holmqvist, E. (2011). *A review of NVE's flood frequency estimation procedures* [Report]. NVE Report 2011-9. https://publikasjoner.nve.no/report/2011/report2011_09.pdf

Winston, R. J., Anderson, A. R., & Hunt, W. F. (2017). Modeling Sediment Reduction in Grass Swales and Vegetated Filter Strips Using Particle Settling Theory. *Journal of Environmental Engineering, 143*(1), 04016075. https://doi.org/10.1061/(ASCE)EE.1943-7870.0001162

Ødegaard, H. (2014). *Water- and wastewater technology (Norwegian title: Vann- og avløpsteknikk)* (2 ed.). Norsk Vann.

## Appendix A: SWMM model results

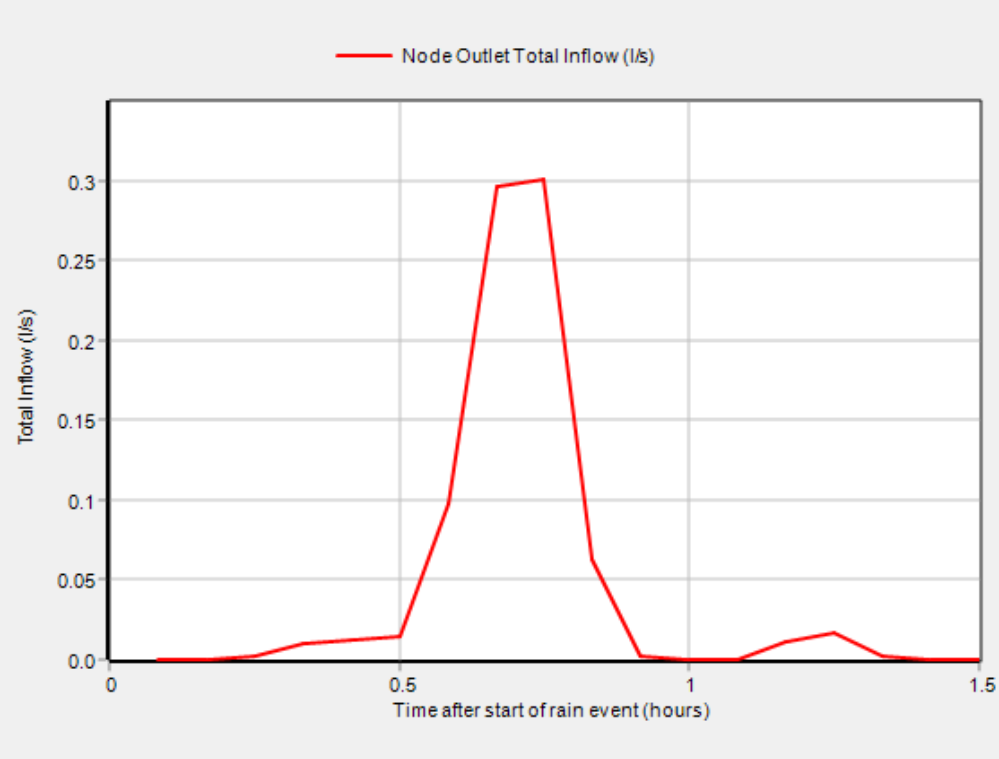


Figure 0.1 Total inflow (l/s) in the outlet node when running a single storm event simulation using a 20-years design rain event without 40% climate factor with a duration of 60 minutes. Max total inflow = 0.3 l/s. (From SWMM).

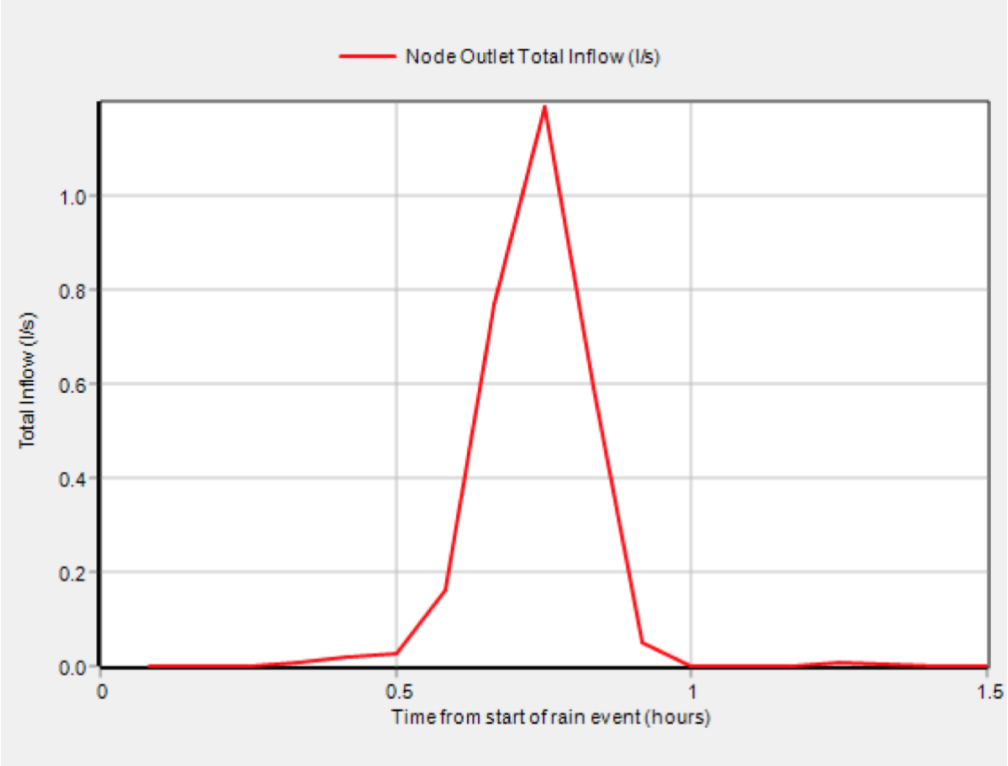


Figure 0.2 Total inflow (l/s) in the outlet node when running a single storm event simulation using a 200-years design rain event without 40% climate factor with a duration of 60 minutes. Max total inflow = 1.19 l/s. (From SWMM).

## Appendix B: R-script for plotting water levels within swale

```
library(ggplot2)
library(reshape)
library(patchwork)

#Set directory
setwd("~/Documents/10_semester_va r2021/R_plot/Swale")
#Import data including precipitation, air temperature and water levels within swale (P2, P3
    , P4)
data <- read.csv("prec+temp+p2+p4+p3_ver17.mai.csv",sep=";", header=TRUE)
#Transform date format
data <- transform(data,PrTime= strptime(Tidspunkt,format="%d.%m.%Y %H:%M"))
data <- transform(data,P2Time= strptime(TimeP2,format="%d.%m.%Y %H:%M"))
data <- transform(data,P4Time= strptime(TimeP4,format="%d.%m.%Y %H:%M"))
data <- transform(data,P3Time= strptime(TimeP3,format="%d.%m.%Y %H:%M"))

data <- subset(data, select=-c(Tidspunkt,TimeP2,TimeP4,TimeP3))

# Create legend
colorsP2 <- c("0.75 m"="blue", "2.23 m"="red", "3.15 m"="dark grey")
colorsP4 <- c("0.75 m"="blue", "2.00 m"="red", "3.00 m"="dark grey")
colorsP3 <- c("0.7 m"="blue", "2.00 m"="red", "3.00 m"="dark grey")

theme_set(theme_bw(base_size = 10))

#Plot precipitation
plotPrecip <- ggplot(data) +
        geom_bar(aes(x=PrTime,y=PrecipInt, color="black", fill= "black"),stat="identity",
    position="identity") +
        guides(fill=FALSE) + guides(color=FALSE) +
        labs(x="", y="Precipitation intensity (mm/h)", title = "Precipitation") +
        scale_x_datetime("", date_breaks = "2 month", date_labels = "%b %y") +
        theme(plot.title = element_text(size = 10, face = "bold"))
#Plot air temperature
plotTemp <- ggplot(data) +
        geom_line(aes(x=PrTime,y=AirTemp),stat="identity", position="identity")  +
        labs(x="", y="Air temperature ( C )", title = "Air temperature") +
        scale_x_datetime("", date_breaks = "2 month", date_labels = "%b %y") +
        theme(plot.title = element_text(size = 10, face = "bold"))
#Plot water levels (P2, P3, P4)
plotP2 <- ggplot(data) +
        geom_line(aes(x=P2Time, y=X0.75m, color="0.75 m")) +
        geom_line(aes(x=P2Time, y=X2.23m, color="2.23 m")) +
        geom_line(aes(x=P2Time, y=X3.15m, color="3.15 m")) +
        labs(x="", y="Water level (m)", color="Sensor depth", title = "Sensor position P2")
    +
        scale_color_manual(values = colorsP2) +
        scale_x_datetime("", date_breaks = "2 month", date_labels = "%b %y") +
        theme(plot.title = element_text(size = 10, face = "bold"))
plotP4 <- ggplot(data) +
        geom_line(aes(x=P4Time,y=X0.75m.1, color="0.75 m")) +
        geom_line(aes(x=P4Time, y=X2m, color="2.00 m")) +
        geom_line(aes(x=P4Time, y=X3m, color="3.00 m")) +
        labs(x="", y="Water level (m)", color="Sensor depth", title = "Sensor position P4")
    +
        scale_color_manual(values = colorsP4) +
        scale_x_datetime("", date_breaks = "2 month", date_labels = "%b %y") +
        theme(plot.title = element_text(size = 10, face = "bold"))
plotP3 <- ggplot(data) +
        geom_line(aes(x=P3Time,y=X0.7m, color="0.7 m")) +
        geom_line(aes(x=P3Time, y=X2m.1, color="2.00 m")) +
        geom_line(aes(x=P3Time, y=X3m.1, color="3.00 m")) +
        labs(x="", y="Water level (m)", color="Sensor depth", title = "Sensor position P3")
    +
        scale_color_manual(values = colorsP3) + scale_x_datetime("", date_breaks = "2 month
    ", date_labels = "%b %y") +
```

```
        theme(plot.title = element_text(size = 10, face = "bold"))

plotP2lim <- plotP2 + coord_cartesian(ylim = c(0, 2.5))
plotP4lim <- plotP4 + coord_cartesian(ylim = c(-0.6, 2))
plotP3lim <- plotP3 + coord_cartesian(ylim = c(-0.6, 2))

#Plot all plots in one figure
plotPrecip/plotTemp/plotP2lim/plotP3lim/plotP4lim
#Save as figure
Figur <- paste("~/Documents/10_semester_va r2021/R_plot/Swale/Figur/Figur_p2+p4+p3_.tiff",
     sep = "")
tiff(Figur, width = 8, height = 10, units = "in", res = 300)
plotPrecip/plotTemp/plotP2lim/plotP3lim/plotP4lim

dev.off()
```

## Appendix C: Water levels within swale (P1, P5 and P6)

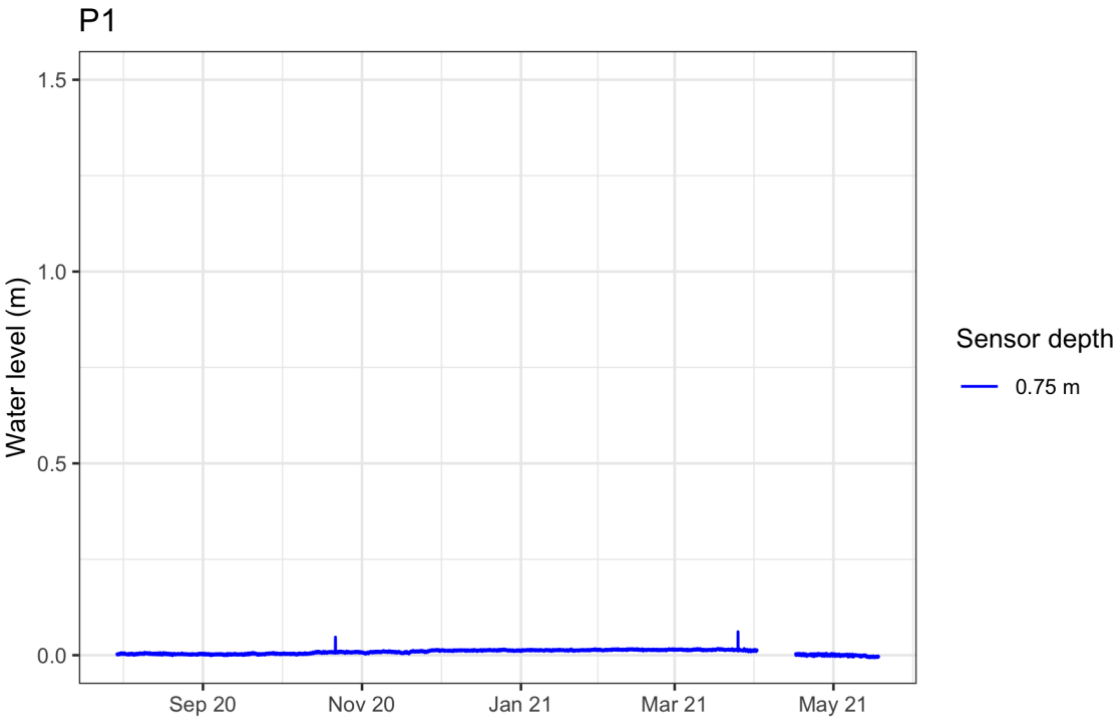


Figure 0.1 Water level within swale in sensor position P1 measured with pressure sensors.

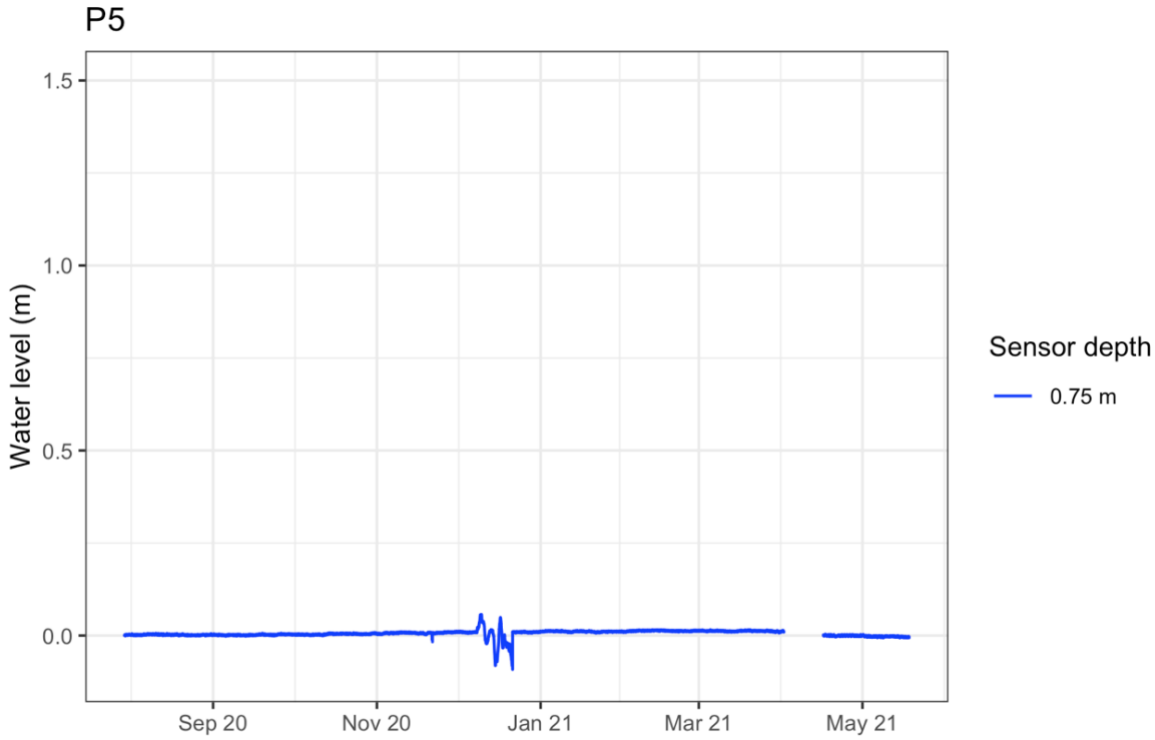


Figure 0.2 Water level within swale in sensor position P5 measured with pressure sensors.

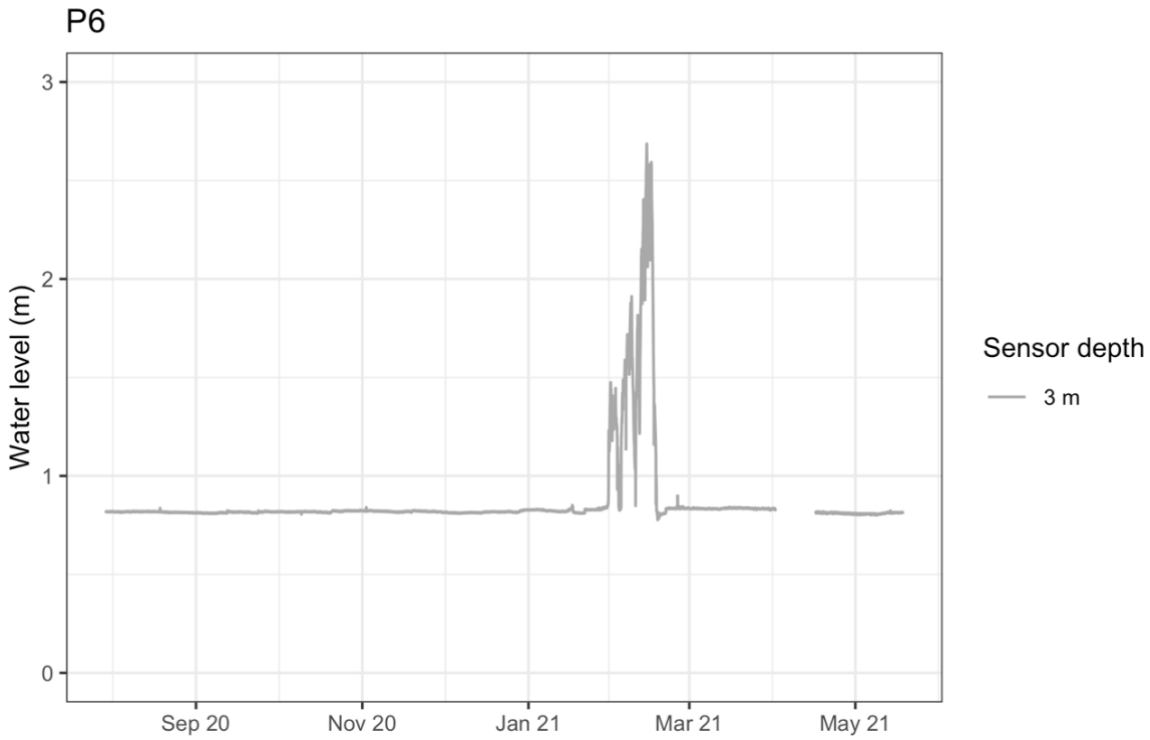

Figure 0.3 Water level within swale in sensor position P6 measured with pressure sensors.

## Appendix D: DDD model input – Parameter files

Table 0.1 Parameter file where a combined regionalisation method (regression and physical similarity).

| | | | |
|---|---|---|---|
| Narsjo | 1 | maxLbog | 951.893 |
| Hypso_area | 1 | midLbog | 534.942 |
| a00 | 204 | bogfrac | 0.0051 |
| a01 | 234 | zsoil | 0.02648 |
| a02 | 261 | zbog | 0.00022 |
| a03 | 284 | NoL | 5 |
| a04 | 299 | cea | 0.01019578 |
| a05 | 313 | R | 0.3 |
| a06 | 334 | Gshape | 1.06863 |
| a07 | 360 | Gscale | 0.019681168 |
| a08 | 393 | GshInt | 1.52948561 |
| a09 | 424 | GscInt | 0.008243772 |
| a10 | 549 | cvHBV | 0.5 |
| pro | 0.1 | Dummy | -1000 |
| vp1 | 0.7 | rv | 1.22117 |
| vp2 | 0.3 | midFl | 3544.863 |
| vt1 | 0.7 | stdFL | 2056.837 |
| vt2 | 0.3 | maxFL | 7594.451 |
| hst1 | 204 | maxDl | 957.079 |
| hst2 | 549 | gtcel | 0.999 |
| hfelt | 317.91 | midDL | 150.055 |
| tgrad | 0 | glacfrac | 0 |
| pgrad | 0 | midGl | 0 |
| pkorr | 1 | stdGl | 0 |
| skorr | 1 | maxGl | 0 |
| TX | 0.5 | g1 | 0 |
| TS | 0 | g2 | 0 |
| CX | 0.05154261 | g3 | 0 |
| CFR | 0.005544869 | g4 | 0 |
| CGLAC | 0.5 | g5 | 0 |
| a0 | 31.92 | g6 | 0 |
| d | 384.1 | g7 | 0 |
| Timeresinsec | 3600 | g8 | 0 |
| MAD | 0.0749687 | g9 | 0 |
| area | 10090000 | g10 | 0 |
| | | CritFux | 160.7 |

Table 0.2 Parameter file where recession and calibration parameters are directly transferred from Fura which is used as single donor.

| | | | |
|---|---|---|---|
| Narsjo | 1 | maxLbog | 951.893 |
| Hypso_area | 1 | midLbog | 534.942 |
| a00 | 204 | bogfrac | 0.0051 |
| a01 | 234 | zsoil | 0.02648 |
| a02 | 261 | zbog | 0.00022 |
| a03 | 284 | NoL | 5 |
| a04 | 299 | cea | 0.01019578 |
| a05 | 313 | R | 0.3 |
| a06 | 334 | Gshape | 0.795 |
| a07 | 360 | Gscale | 0.038 |
| a08 | 393 | GshInt | 1.002 |
| a09 | 424 | GscInt | 0.018 |
| a10 | 549 | cvHBV | 0.5 |
| pro | 0.1 | Dummy | -1000 |
| vp1 | 0.7 | rv | 1.22117 |
| vp2 | 0.3 | midFl | 3544.863 |
| vt1 | 0.7 | stdFL | 2056.837 |
| vt2 | 0.3 | maxFL | 7594.451 |
| hst1 | 204 | maxDl | 957.079 |
| hst2 | 549 | gtcel | 0.999 |
| hfelt | 317.91 | midDL | 150.055 |
| tgrad | 0 | glacfrac | 0 |
| pgrad | 0 | midGl | 0 |
| pkorr | 1 | stdGl | 0 |
| skorr | 1 | maxGl | 0 |
| TX | 0.5 | g1 | 0 |
| TS | 0 | g2 | 0 |
| CX | 0.05154261 | g3 | 0 |
| CFR | 0.005544869 | g4 | 0 |
| CGLAC | 0.5 | g5 | 0 |
| a0 | 31.92 | g6 | 0 |
| d | 384.1 | g7 | 0 |
| Timeresinsec | 3600 | g8 | 0 |
| MAD | 0.0749687 | g9 | 0 |
| area | 10090000 | g10 | 0 |
| | | CritFux | 160.7 |

## Appendix E: R-script for plotting water stage, “observed” discharge and simulated discharge in Stabekken

```
library(ggplot2)
library(reshape)
library(patchwork)

#Set directory
setwd("~/Documents/10_semester_va r2021/R_plot/Diver")
#Import data including measured water stage in Stabekken and "observed" discharge
data <- read.csv("stage+discharge_nov-mai_heltUjan.csv",sep=";", header=TRUE)
#Transform date format
data <- transform(data,TimeUpstream= strptime(TimeUp,format="%d.%m.%Y %H:%M"))
data <- transform(data,TimeDownstream= strptime(TimeDown,format="%d.%m.%Y %H:%M"))

data <- subset(data, select=-c(TimeUp, TimeDown))

#Create legend
location <- c("Upstream TD-Diver ID:AZ095"="dark blue", "Downstream TD-Diver ID:AZ173"="red
    ")

theme_set(theme_bw(base_size = 10))
#Plot water stage in Stabekken
plotDiver <- ggplot(data) +
  geom_line(aes(x=TimeUpstream,y=Upstream, color="Upstream TD-Diver ID:AZ095"), stat = "
    identity", position = "identity", show.legend = FALSE) +
  geom_line(aes(x=TimeDownstream,y=Downstream, color="Downstream TD-Diver ID:AZ173"), stat
    = "identity", position = "identity", show.legend = FALSE) +
  labs(x="", y="Water level (cm)", color="", title = "Observed water stage") +
  scale_x_datetime("", date_breaks = "1 month", date_labels = "%b %y")  +
  scale_color_manual(values = location)  +
  theme(plot.title = element_text(size = 10, face = "bold"))

#Plot "observed" discharge
plotDischarge <- ggplot(data) +
  geom_line(aes(x=TimeUpstream,y=Discharge_Up, color="Upstream TD-Diver ID:AZ095"), stat =
    "identity", position = "identity") +
  geom_line(aes(x=TimeDownstream,y=Discharge_Down, color="Downstream TD-Diver ID:AZ173"),
    stat = "identity", position = "identity") +
  labs(x="", y="Discharge (m3/s)", color="", title = "Discharge transformed from the
    observed water stage") +
  scale_x_datetime("", date_breaks = "1 month", date_labels = "%b %y") +
  scale_color_manual(values = location) +
  theme(plot.title = element_text(size = 10, face = "bold")) +
  theme(legend.position = "bottom")

#Import simulated discharge data
dataDDD <- read.csv("Simulated discharge-nov2020-mai2021.csv",sep=";", header=TRUE)
#Transform date format
dataDDD <- transform(dataDDD,TimeDate= strptime(TimeDDD,format="%d.%m.%Y %H:%M"))
#Plot simulated discharge
plotDDD <- ggplot(dataDDD) +
  geom_line(aes(x=TimeDate,y=Sim_discharge), stat = "identity", position = "identity") +
  geom_line(aes(x=TimeDate,y=Sim_discharge), stat = "identity", position = "identity") +
  labs(x="", y="Discharge (m3/s)", title = "Simulated discharge using the DDD model") +
  scale_x_datetime("", date_breaks = "1 month", date_labels = "%b %y") +
  theme(plot.title = element_text(size = 10, face = "bold"))

#Import climate data (precipitation and air temperature)
dataPrecip <- read.csv("precip+temp_nov-mai.csv",sep=";", header=TRUE)
#Transform date format
dataPrecip <- transform(dataPrecip,PrTime= strptime(Tidspunkt,format="%d.%m.%Y %H:%M"))
#Plot precipitation and air temperature
plotPrecip <- ggplot(dataPrecip) +
  geom_bar(aes(x=PrTime,y=PrecipInt, color="black", fill= "black"),stat="identity",
    position="identity") +
  guides(fill=FALSE) + guides(color=FALSE) + labs(x="", y="Precipitation intensity (mm/h)",
```

```
      title = "Precipitation") +
  scale_x_datetime("", date_breaks = "1 month", date_labels = "%b %y")  +
  theme(plot.title = element_text(size = 10, face = "bold"))

plotTemp <- ggplot(dataPrecip) +
  geom_line(aes(x=PrTime,y=AirTemp),stat="identity", position="identity")  +
  labs(x="", y="Air temperature ( C )", title = "Air temperature") +
  scale_x_datetime("", date_breaks = "1 month", date_labels = "%b %y")  +
  theme(plot.title = element_text(size = 10, face = "bold"))

#Plot all plots in one figure
plotPrecip/plotTemp/plotDiver/plotDischarge/plotDDD
#Save as figure
Figur <- paste("~/Documents/10_semester_va r2021/R_plot/Diver/Figur/Figur_prec+temp+
    waterlevel+discharge+simulatedDischarge.tiff", sep = "")
tiff(Figur, width = 8, height = 10, units = "in", res = 300)
plotPrecip/plotTemp/plotDiver/plotDischarge/plotDDD

dev.off()
```

NTNU

Kunnskap for en bedre verden